On the convergence of the fictitious domain method for wave equation problems

Eliane Bécache, Jerónimo Rodríguez, Chrysoula Tsogka

▶ **To cite this version:**

Eliane Bécache, Jerónimo Rodríguez, Chrysoula Tsogka. On the convergence of the fictitious domain method for wave equation problems. [Research Report] RR-5802, INRIA. 2006, pp.37. ⟨inria-00070222⟩

HAL Id: inria-00070222

https://inria.hal.science/inria-00070222v1

Submitted on 19 May 2006

HAL is a multi-disciplinary open access archive for the deposit and dissemination of scientific research documents, whether they are published or not. The documents may come from teaching and research institutions in France or abroad, or from public or private research centers.

L'archive ouverte pluridisciplinaire **HAL**, est destinée au dépôt et à la diffusion de documents scientifiques de niveau recherche, publiés ou non, émanant des établissements d'enseignement et de recherche français ou étrangers, des laboratoires publics ou privés.

HAL Authorization

INRIA

INSTITUT NATIONAL DE RECHERCHE EN INFORMATIQUE ET EN AUTOMATIQUE

On the convergence of the fictitious domain method for wave equation problems

E. Bécache — J. Rodríguez — C. Tsogka

N° 5802

Janvier 2006

Thème NUM

ISSN 0249-6399 ISRN INRIA/RR--5802--FR+ENG

INRIA
ROCQUENCOURT

On the convergence of the fictitious domain method for wave equation problems

E. Bécache* , J. Rodríguez† , C. Tsogka‡

Thème NUM —Systèmes numériques
Projet POEMS

Rapport de recherche n° 5802 —Janvier 2006 —37 pages

Abstract: This paper deals with the convergence analysis of the fictitious domain method used for taking into account the Neumann boundary condition on the surface of a crack (or more generally an object) in the context of acoustic and elastic wave propagation. For both types of waves we consider the first order in time formulation of the problem known as mixed velocity-pressure formulation for acoustics and velocity-stress formulation for elastodynamics. The convergence analysis for the discrete problem depends on the mixed finite elements used. We consider here two families of mixed finite elements that are compatible with mass lumping. When using the first one which is less expensive and corresponds to the choice made in a previous paper, it is shown that the fictitious domain method does not always converge. For the second one a theoretical convergence analysis is presented in the acoustic case and numerical convergence is shown both for acoustic and elastic waves.

Key-words: mixed finite elements, fictitious domain method, acoustic waves, elastic waves, convergence

* POEMS, INRIA-Rocquencourt, BP 105, F-78153 Le Chesnay Cédex (eliane.becache@inria.fr)
† POEMS, ENSTA, 32 boulevard Victor, 75739 Paris cedex 15, France (jeronimo.rodriguez@inria.fr)
‡ University of Chicago, Dept. Mathematics, 5734 University Avenue Chicago, IL 60637, USA (tsogka@math.uchicago.edu)

Unité de recherche INRIA Rocquencourt
Domaine de Voluceau, Rocquencourt, BP 105, 78153 Le Chesnay Cedex (France)
Téléphone : +33 1 39 63 55 11 —Télécopie : +33 1 39 63 53 30

Sur la convergence des domaines fictifs pour des problèmes d'ondes

Résumé : Cet article concerne l'analyse de convergence de la méthode des domaines fictifs utilisée pour prendre en compte une condition aux limites de Neumann sur la surface d'une fissure (ou plus généralement d'un obstacle) dans le context de la propagation d'ondes acoustiques et élastiques. Pour les deux types d'ondes, on consideère la formulation du premier ordre en temps du problème, appelée formulation mixte vitesse-pression pour l'acoustique et formulation mixte vitesse-contraintes pour l'élastodynamique. L'analyse de convergence du problème discret dépend des éléments finis mixtes utilisés. Nous considérons ici deux familles d'éléments finis mixtes compatibles avec la condensation de masse. Quand on utilise le premier choix qui est moins couteux et correspond au choix fait dans un papier antérieur, il est montré que la méthode des domaines fictifs ne converge pas toujours. Pour le second choix, une analyse théorique de convergence de la méthode est présentée dans le cas acoustique et la convergence numérique est montrée pour les deux cas acoustique et élastodynamique.

Mots-clés : éléments finis mixtes, méthode des domaines fictifs, ondes acoustiques, ondes élastiques, convergence

Contents

1 Introduction

This work falls within the more general framework of developing efficient numerical methods for approximating wave propagation in complex media such as anisotropic, heterogeneous media with cracks or objects of arbitrary shapes. We consider here scattering of acoustic and elastic waves by perfect reflectors, *i.e.*, objects or cracks with a homogeneous Neumann boundary condition. To solve these wave propagation problems in an efficient way we use a fictitious domain approach. This approach, also called the domain embedding method, consists in extending artificially the solution inside the object so that the new domain of computation has a very simple shape (typically a rectangle in 2D). To account for the boundary condition, a new auxiliary unknown, defined only at the boundary of the object, is introduced. The solution of this extended problem has now a singularity across the boundary of the object which can be related to the new unknown. The main advantage of the method is that the mesh for the solution on the enlarged domain can be chosen independently of the geometry of the object. In particular, one can use regular grids or structured meshes which allows for simple and efficient computations.

Special interest has been given to this approach as it has been shown to lead to efficient numerical methods for a large number of applications (e.g [1, 21, 16, 13, 15, 18, 19]) and these last years for time dependent wave propagation problems ([10, 12, 23, 20, 5, 2]). The method can be re-interpreted in terms of optimization theory in which case the auxiliary unknown appears as a Lagrange multiplier associated to the boundary condition viewed now as an equality constraint in the functional space. Thus the key point of the approach is that it

can be applied to essential type boundary conditions, *i.e.*, conditions that can be considered as an equality constraint.

To do so with the free surface condition, the dual unknown (velocity in the acoustic case and stress tensor in the elastic) has to be one of the unknowns. This can be done by considering either the dual formulation (the formulation with only one unknown, the dual one) or the mixed dual primal formulation. In both cases, the dual unknown is introduced and seeked for in the space $H(\mathrm{div})$ in which the Neumann boundary condition $\mathbf{v} \cdot n$ or $\boldsymbol{\sigma} \cdot n = 0$ can be considered as an equality constraint. In this case, the Lagrange multiplier is nothing but the jump of the primal unknown across the boundary of the object.

For the approximation of the mixed formulation in the scalar acoustic case, in [4], the authors have proposed mixed finite elements, the so-called $Q_{k+1}^{div} - Q_k$ elements, inspired by Nédélec's second family [22]. These elements are compatible with mass lumping, and therefore allow for constructing explicit schemes in time. The generalization of those elements in the case of elastic waves was introduced in [3] for the velocity-stress formulation. The above elements have been used for solving diffraction problems in complex media due to the fictitious domain method in [5].

A non standard convergence analysis of the $Q_{k+1}^{div} - Q_k$ elements has been carried out in [4] for their scalar version and in [6] for their elastodynamic vectorial version. However this convergence analysis only deals with the velocity-pressure (resp. velocity-stress) mixed problem without object, that is, it did not concern the convergence of the fictitious domain method.

In this paper the convergence of the fictitious domain method is analyzed. The scalar case is considered first. Section 2 presents the fictitious domain method and its approximation. In section 3, we address the question of its convergence when using the $Q_1^{div} - Q_0$ elements for approximating the volume unknown and it is shown in section 3.2 through some numerical experiments that the method does not always converge.

Motivated by this negative result, we introduce in section 4 a modified finite element, the so-called $Q_1^{div} - P_1^{disc}$. After illustrating with numerical results the convergence for this modified element in section 4.2, we present its dispersion analysis in section 4.3. This analysis shows in particular the presence of spurious modes due to the enrichment of the approximation space for the primal unknown (the pressure for the scalar case and the velocity for the elastic case). To get rid of this non physical part of the solution we propose to attenuate the spurious modes in section 4.4 by introducing a damping term in the equations. Section 5 is devoted to the convergence analysis of the fictitious domain method when using the $Q_1^{div} - P_1^{disc}$ element. The theoretical order of convergence is compared to the numerical one in section 6 for a particular object. In a second part, the vectorial elastic case is considered. The convergence issues are the same as in the scalar case, but the proof of convergence is not a straightforward generalization of this simplified case, as explained in section 7. However, numerical results shown in section 8 and the numerical order of convergence obtained in section 9 for a particular case, seem to confirm the conjecture that the modified element still converges in the elastic case.

2 The fictitious domain formulation of the diffraction problem. The acoustic case

2.1 The continuous problem

We consider the diffraction of an acoustic wave by an object with a Neumann type condition for the pressure field on its boundary Γ. The object can be either an obstacle with a closed boundary or a crack with an open boundary (see Fig. 1) but for the sake of clarity we will consider here only this second configuration. The domain of propagation is denoted Ω with an exterior boundary Σ (see Fig. 1) and we assume that $C = \Omega \cup \Gamma$ is a domain of "simple" geometry, typically a rectangle.

The propagation medium is assumed to be anisotropic and the equation satisfied by the pressure field is the scalar wave equation. In order to apply the fictitious domain method to this type of boundary condition it is

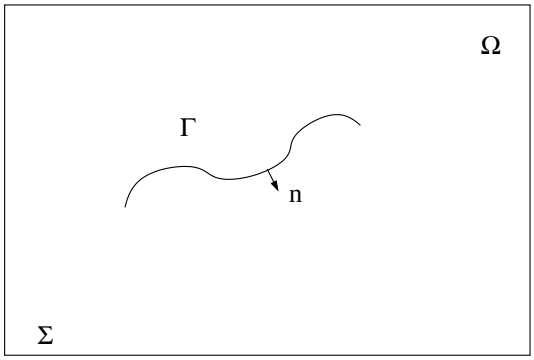

Figure 1: Geometry of the problem.

classical (e.g. [4]) to formulate the problem as a first-order velocity-pressure system,

$$(1)\qquad \left\{\begin{array}{l} \text{Find } (\mathbf{v},p) : (x,t)\in\Omega\times[0,T]\mapsto(\mathbf{v}(x,t),p(x,t))\in\mathbb{R}^2\times\mathbb{R} \text{ satisfying,} \\ \rho\dfrac{\partial p}{\partial t} - \operatorname{div}\mathbf{v} = f, \quad \text{in } \Omega, \quad (a) \\ \mathbf{A}\dfrac{\partial \mathbf{v}}{\partial t} - \nabla p = 0, \quad \text{in } \Omega, \quad (b) \\ \mathbf{v}\cdot n = 0, \quad \text{on } \Gamma, \quad (c) \\ p = 0, \quad \text{on } \Sigma, \quad (d) \end{array}\right.$$

with the initial conditions,

$$(2)\qquad \left\{\begin{array}{l} p(t=0) = p_0, \\ \mathbf{v}(t=0) = \mathbf{v}_0, \end{array}\right.$$

where the unknowns p and $\mathbf{v}$ denote the pressure and the velocity field. The scalar function ρ and the tensor $\mathbf{A}$ characterize the propagation medium and f represents the external forces. Moreover, we assume that ρ satisfies

$$0<\rho^-\le\rho(x)\le\rho^+<+\infty,$$

and $\mathbf{A}$ is a second order symmetric positive tensor such that

$$0<\kappa|\mathbf{w}|^2\le\mathbf{A}(x)\mathbf{w}\cdot\mathbf{w}\le\nu|\mathbf{w}|^2 \quad \forall\mathbf{w}\neq 0.$$

We also assume that the support of the initial data $(\mathbf{v}_0,p_0)$ and the support of the source f do not intersect Γ, which means that

$$(3)\qquad \operatorname{supp}(\mathbf{v}_0)\cup\operatorname{supp}(p_0)\subset C\setminus\Gamma, \quad \bigcup_{t\le T}\operatorname{supp}(f(t))\subset C\setminus\Gamma.$$

The *natural* variational formulation of this problem would be set in some functional spaces that depend on the shape of the obstacle (i.e., depend on Ω). More precisely, the classical variational formulation is,

$$(4)\qquad \left\{\begin{array}{l} \text{Find } (\mathbf{v}(t),p(t))\in \underline{X}_0\times M \text{ satisfying,} \\ \dfrac{\mathrm{d}}{\mathrm{d}t}\displaystyle\int_\Omega \mathbf{A}\mathbf{v}\cdot\mathbf{w}\,\mathrm{d}x + \int_\Omega \operatorname{div}(\mathbf{w})p\,\mathrm{d}x = 0, \quad \forall\mathbf{w}\in\underline{X}_0, \\ \dfrac{\mathrm{d}}{\mathrm{d}t}\displaystyle\int_\Omega \rho pq\,\mathrm{d}x - \int_\Omega \operatorname{div}(\mathbf{v})q\,\mathrm{d}x = (f,q), \quad \forall q\in M, \\ (\mathbf{v},p)_{/t=0} = (\mathbf{v}_0,p_0), \end{array}\right.$$

where the functional spaces are defined as,

$$\underline{X}_0(\Omega) = \{\mathbf{w} \in H(\mathrm{div};\Omega),\ \mathbf{w}\cdot\mathbf{n} = 0,\ \text{ on } \Gamma\},\ M = L^2(\Omega).$$

The well posedness of problem (4) results from classical theory on hyperbolic PDEs,

Theorem 2.1 *Let $f \in C^0([0,T],M)$, $\mathbf{v}_0 \in \underline{X}_0(\Omega)$, $p_0 \in M$ satisfying (3). Then, problem (4) has a unique solution $(\mathbf{v},p) \in (C^1([0,T],(L^2(\Omega))^2) \cap C^0([0,T],\underline{X}_0(\Omega))) \times C^1([0,T],M)$.*

The fictitious domain formulation of this problem consists in taking into account the boundary condition on Γ in a weak way, by introducing a Lagrange multiplier λ defined on Γ. This allows for working in functional spaces (for the volume unknowns) which do not depend any more on the shape of the obstacle. The fictitious domain formulation is then the following, (to simplify the notations, we still denote by $(\mathbf{v}(t),p(t))$ the new unknowns defined now in C)

$$\left\{\begin{array}{l} \text{Find } (\mathbf{v}(t),p(t),\lambda(t)) \in \underline{X}\times M\times\mathcal{G} \text{ satisfying,}\\ \dfrac{\mathrm{d}}{\mathrm{d}t}a(\mathbf{v},\mathbf{w}) + b(\mathbf{w},p) - <\mathbf{w}\cdot\mathbf{n},\lambda>_\Gamma = 0, \quad \forall \mathbf{w}\in\underline{X},\\ \dfrac{\mathrm{d}}{\mathrm{d}t}(p,q)_\rho - b(\mathbf{v},q) = (f,q), \quad \forall q\in M,\\ <\mathbf{v}\cdot\mathbf{n},\mu>_\Gamma = 0, \quad \forall \mu\in\mathcal{G},\\ (\mathbf{v},p)_{/t=0} = (\mathbf{v}_0,p_0), \end{array}\right. \tag{5}$$

where the functional spaces are now defined as,

$$\underline{X}(=\underline{X}(C)) = H(\mathrm{div};C),\ M = L^2(C),\ \mathcal{G} = H^{1/2}_{00}(\Gamma),$$

the bilinear forms as,

$$\left\{\begin{array}{lll} a(\mathbf{v},\mathbf{w}) &=& \displaystyle\int_C \mathbf{A}\mathbf{v}\cdot\mathbf{w}\,\mathrm{d}x, \quad \forall(\mathbf{v},\mathbf{w})\in\underline{X}\times\underline{X},\\ (p,q)_\eta &=& \displaystyle\int_C \eta\, p\, q\,\mathrm{d}x, \quad \forall(p,q)\in M\times M,\\ b(\mathbf{w},q) &=& \displaystyle\int_C \mathrm{div}(\mathbf{w}) q\,\mathrm{d}x, \quad \forall(\mathbf{w},q)\in\underline{X}\times M, \end{array}\right. \tag{6}$$

and the bracket $<\mathbf{w}\cdot\mathbf{n},\mu>_\Gamma$ is the duality product between $\mathcal{G}$ and $\mathcal{G}'$. Note that, due to (3), under assumptions of theorem 2.1, the data also belong to,

$$f \in C^0([0,T],M), \quad \mathbf{v}_0 \in \underline{X}(C), \quad p_0 \in M. \tag{7}$$

In the following we will denote by $(\cdot,\cdot) := (\cdot,\cdot)_1$ the usual $L^2(C)$ scalar product.

The well posedness of problem (5) follows from the three following lemmas.

Lemma 2.1 *(Existence) We assume the data $(\mathbf{v}_0,p_0,f)$ satisfy (7). Let $(\mathbf{v},p) \in (C^1([0,T],(L^2(\Omega))^2) \cap C^0([0,T],\underline{X}_0(\Omega))) \times C^1([0,T],M)$ be the solution of problem (4). Then:*
(i) $p \in C^0([0,T],H^1(\Omega))$ and one can define

$$\lambda = [p]_\Gamma \in C^0([0,T],\mathcal{G}),$$

where $[p]_\Gamma$ denotes the jump of p across Γ.
(ii) $\mathbf{v} \in C^0([0,T],\underline{X}(C))$ and $(\mathbf{v},p,\lambda)$ is a solution of (5).

Proof. (i) If $(\mathbf{v},p) \in (C^1([0,T],(L^2(\Omega))^2) \cap C^0([0,T],\underline{X}_0(\Omega))) \times C^1([0,T],M)$ is the solution of (4), the re-interpretation of the variational formulation shows that it satisfies in particular (1)-(b) in $(L^2(\Omega))^2$. Since $\partial_t v \in C^0([0,T],(L^2(\Omega))^2)$ we deduce that $\nabla p \in C^0([0,T],(L^2(\Omega))^2)$ and therefore $p \in C^0([0,T],H^1(\Omega))$. It is then possible to define its trace on Γ and define λ.
(ii) $\mathbf{v}$ is in $C^0([0,T],\underline{X}_0(\Omega))$ and by definition of $\underline{X}_0(\Omega)$ it satisfies $\mathbf{v}\cdot\mathbf{n}=0$ on Γ which implies in particular that $\mathbf{v}\cdot\mathbf{n}$ is continuous through Γ thus $\mathbf{v} \in C^0([0,T],\underline{X}(C))$. Again using the re-interpretation of the variational formulation, one can see that (1)-(a) is satisfied in $L^2(\Omega)$, (1)-(b) in $(L^2(\Omega))^2$ and (1)-(d) in $H^{1/2}(\Sigma)$. We then easily check that it satisfies (5), by multiplying (1)-(a) with a function $q \in M$, (1)-(b) with a function $\mathbf{w} \in \underline{X}$, integrating by parts and using the definition of λ. □

Lemma 2.2 *(Energy identity). If $(\mathbf{v},p,\lambda)$ is a solution of (5), the energy*

$$\mathcal{E} = \frac{1}{2}a(\mathbf{v},\mathbf{v}) + \frac{1}{2}\|p\|_\rho^2,$$

satisfies the following identity,

$$\frac{d\mathcal{E}}{dt} = (f,p). \tag{8}$$

Lemma 2.3 *The following inf-sup condition is satisfied,*

$$\exists k>0,\ \forall \mu \in \mathcal{G},\ \exists \mathbf{w} \in \underline{X},\ <\mathbf{w}\cdot\mathbf{n},\mu>_\Gamma \geq k\,\|\mu\|_{\mathcal{G}}\,\|\mathbf{w}\|_{\underline{X}}. \tag{9}$$

Proof. This result has been proved in [20] for a closed obstacle $\widetilde{\Gamma}$, and the corresponding space $\widetilde{\mathcal{G}} = H^{1/2}(\widetilde{\Gamma})$. It is straightforward to adapt the proof to the present case, extending the open curve Γ to a closed curve $\widetilde{\Gamma}$, since for any function $\mu \in H^{1/2}_{00}(\Gamma)$ one can define its extension by zero $\widetilde{\mu} \in H^{1/2}(\widetilde{\Gamma})$. We then apply the result for $\widetilde{\mu}$ and using $\|\widetilde{\mu}\|_{\widetilde{\mathcal{G}}} = \|\mu\|_{\mathcal{G}}$ we obtain the result for μ. □

Theorem 2.2 *Let $f \in C^0([0,T],M)$, $\mathbf{v}_0 \in \underline{X}$, $p_0 \in M$ satisfying (3). Problem (5) admits a unique solution $(\mathbf{v},p,\lambda) \in (C^1([0,T],(L^2(C))^2) \cap C^0([0,T],\underline{X})) \times C^1([0,T],M) \times C^0([0,T],\mathcal{G})$.*

Proof. The existence follows from lemma 2.1. The energy identity (8) implies the uniqueness of $(\mathbf{v},p)$ and the uniqueness of λ is a consequence of the inf-sup condition (9). □

Remark 1 On the regularity of the solution. *For regular data, one can expect more regularity on the solution. However, in general, the space regularity of the volumic part of the solution is at most,*

$$\mathbf{v}(t) \ \in\ H^{\frac{1}{2}-\varepsilon}(\mathrm{div},C), \quad p(t) \in H^{\frac{1}{2}-\varepsilon}(C), \qquad \varepsilon>0,$$

and this is obtained for regular enough data and a regular geometry of the crack. This is due to the fact that the unknowns are defined on the whole domain C without considering the geometry of the obstacle.

The regularity in Ω (i.e. outside the obstacle) is in general higher and depends on the geometry of the obstacle. In particular, for data $(\mathbf{v}_0,p_0,f)$ satisfying (7), we have

- *for a closed boundary:*
$$p_{/\Omega}(t) \in H^2(\Omega), \quad \lambda(t) \in H^{3/2}(\Gamma)$$
- *for an open boundary, due to the singular behavior near the tip of the crack [17] (the solution behaves as $\sqrt{r}$, r being here the distance to the tip), we have*
$$p_{/\Omega}(t) \in H^{3/2-\varepsilon}(\Omega), \quad \lambda(t) \in H^{1-\varepsilon}(\Gamma), \qquad \varepsilon>0.$$

2.2 The semi-discrete approximation

For the approximation in space of this problem, we introduce finite dimensional spaces $\underline{X_h} \subset \underline{X}$, $M_h \subset M$ and $\mathcal{G}_H \subset \mathcal{G}$ satisfying the approximation properties,

$$
\left|
\begin{array}{rcll}
\lim\limits_{h\to 0} \inf\limits_{\mathbf{w}_h \in \underline{X_h}} \|\mathbf{v}-\mathbf{w}_h\|_{\underline{X}} & = & 0, & \forall \mathbf{v} \in \underline{X}, \\
\lim\limits_{h\to 0} \inf\limits_{q_h \in M_h} \|p-q_h\|_{M} & = & 0, & \forall p \in M, \\
\lim\limits_{H\to 0} \inf\limits_{\mu_H \in \mathcal{G}_H} \|\lambda-\mu_H\|_{\mathcal{G}} & = & 0, & \forall \lambda \in \mathcal{G}.
\end{array}
\right. \tag{10}
$$

The semi-discrete problem is then,

$$
\left\{
\begin{array}{l}
\text{Find } (\mathbf{v}_h(t), p_h(t), \lambda_H(t)) \in \underline{X_h} \times M_h \times \mathcal{G}_H \text{ such that,} \\
\dfrac{\mathrm{d}}{\mathrm{d}t} a(\mathbf{v}_h, \mathbf{w}_h) + b(\mathbf{w}_h, p_h) - < \mathbf{w}_h \cdot \mathbf{n}, \lambda_H >_\Gamma = 0, \qquad \forall \mathbf{w}_h \in \underline{X_h}, \\
\dfrac{\mathrm{d}}{\mathrm{d}t} (p_h, q_h)_\rho - b(\mathbf{v}_h, q_h) = (f, q_h), \quad \forall q_h \in M_h, \\
< \mathbf{v}_h \cdot \mathbf{n}, \mu_H >_\Gamma = 0, \qquad \forall \mu_H \in \mathcal{G}_H, \\
\mathbf{v}_h(t=0) = \mathbf{v}_{h,0}, \\
p_h(t=0) = p_{h,0},
\end{array}
\right. \tag{11}
$$

where $(\mathbf{v}_{h,0}, p_{h,0}) \in X_h \times M_h$ is an approximation of the exact initial condition.

The question is : how to choose the approximate spaces in order to insure the convergence of $(\mathbf{v}_h, p_h, \lambda_H)$ to $(\mathbf{v}, p, \lambda)$?

3 The fictitious domain method using the $Q_1^{div} - Q_0$ element

3.1 Position of the problem

For the volumic unknowns, we introduce a regular mesh $\mathcal{T}_h$ of the rectangular domain C composed of square elements of length h. In [4], we introduced for the problem without obstacle new mixed finite elements, the so-called $Q_{k+1}^{div} - Q_k$ elements, inspired by Nédélec's second family [22]. These elements are compatible with mass lumping, and therefore allow for constructing an explicit scheme in time. A non standard convergence analysis of these $Q_{k+1}^{div} - Q_k$ elements has been carried out, showing the convergence without the fictitious domain method. Our first choice for the approximation spaces of the problem with an obstacle was naturally the lowest order element $Q_1^{div} - Q_0$ for the velocity and the pressure fields,

$$
\left\{
\begin{array}{l}
\underline{X_h} = \{\mathbf{w}_h \in \underline{X} \,/\, \forall K \in \mathcal{T}_h,\ \mathbf{w}_h|_K \in Q_1 \times Q_1\}, \\
\\
M_h = M_h^0 \quad \text{with} \quad M_h^0 = \{q_h \in M \,/\ \forall K \in \mathcal{T}_h,\ q_h|_K \in Q_0\}.
\end{array}
\right. \tag{12}
$$

The degrees of freedom for the velocity are described in Figure 2. For more details on this element we refer to [4]. Notice that the velocity approximation space $\underline{X_h}$ contains the lower order Raviart Thomas element,

$$
\underline{X_h}^{RT} = \{\mathbf{w}_h \in \underline{X} \,/\, \forall K \in \mathcal{T}_h,\ \mathbf{w}_h|_K \in P_{10} \times P_{01}\}.
$$

For the approximation of the Lagrange multiplier, we introduce a mesh of Γ composed of N curvilinear segments S_j of length H_j, and we set $H = \sup_j H_j$. We assume that this mesh is uniformly regular,

$$
\exists \nu,\ 0 < \nu \leq 1, \text{ such that } : \forall j,\ 1 \leq j \leq N,\ H_j \geq \nu H. \tag{13}
$$

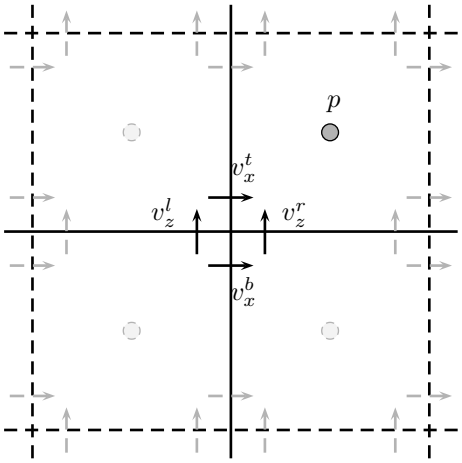

Figure 2: Degrees of freedom for the $Q_1^{div} \times Q_0$ mixed finite element.

We then choose the space of continuous linear piecewise functions:

$$\mathcal{G}_H = \left\{ \nu_H \in \mathcal{G} \,/\, \forall S_j,\ j = 1, \ldots, N,\ \nu_H\big|_{S_j} \in P_1 \right\}. \tag{14}$$

The spaces $(\underline{X_h}, M_h^0, \mathcal{G}_H)$ clearly satisfy the approximation properties (10). This choice which seemed to us natural, since the convergence was proven without obstacle, is the one that was used in [5] for the more complex elastodynamic case. However we have not been able to prove the convergence of the fictitious domain method with these spaces.

The convergence analysis of the fictitious domain method applied to other problems [1, 13, 20] shows that convergence holds if a compatibility condition between the step sizes of the two meshes is satisfied,

$$H \geq \alpha h. \tag{15}$$

We will show in what follows some numerical illustrations which seem to indicate that for some special configurations of obstacles, the method does not converge.

Before showing these numerical results, let us briefly recall the main difficulty of the convergence analysis in the case without object. Introducing the linear operators,

$$\begin{array}{rcccccl} B: & \underline{X} & \longrightarrow & M' & & & \\ & \mathbf{w} & \mapsto & B(\mathbf{w}): & M & \longrightarrow & \mathbb{R} \\ & & & & q & \mapsto & < B(\mathbf{w}), q >= b(\mathbf{w}, q) \end{array}$$

$$\begin{array}{rcccccl} B_h: & \underline{X_h} & \longrightarrow & M_h' & & & \\ & \mathbf{w}_h & \mapsto & B_h(\mathbf{w}_h): & M_h & \longrightarrow & \mathbb{R} \\ & & & & q_h & \mapsto & < B_h(\mathbf{w}_h), q_h >= b(\mathbf{w}_h, q_h) \end{array}$$

it is easy to verify that the inclusion

$$\text{Ker}(B_h) \subset \text{Ker}(B), \tag{16}$$

is not satisfied and that furthermore the bilinear form $a(.,.)$ is not coercive on $\text{Ker}(B_h)$ (even if it is on $\text{Ker}(B)$), so that our problem does not fit the classical mixed finite element theory (cf. [8, 14]). It was however possible to overcome this difficulty when dealing with the problem without fictitious domain method. When coupled with the fictitious domain method, the same technique cannot be applied.

3.2 Numerical illustrations

The computational domain is the square $[0,10]mm \times [0,10]mm$ composed by an homogeneous isotropic material with $\rho = 1000$Kgr/m^3 and $\mathbf{A} = I \times 10^9$Pa. It is excited by an initial condition on the pressure centered on $(x_c, z_c) = (5,5)$mm,

$$p((x,z),t=0) \quad = \quad 0.1\ F\left(\frac{r}{r_0}\right),$$

where $F(r)$ is supported in $[0,1]$ and given by (for $r \in [0,1]$)

$$F(r) \quad = \quad A_0 - A_1\cos(2\pi r) + A_2\cos(3\pi r) - A_3\cos(6\pi r),$$

with $\mathbf{r} = (x - x_c, z - z_c)^t$, $r = \|\mathbf{r}\|$, $r_0 = 1$mm and

$$A_0 = 0.35875, \quad A_1 = 0.48829, \quad A_2 = 0.14128, \quad A_3 = 0.01168.$$

We consider a uniform mesh of squares using a discretization step $h = 0.025$mm. The time discretization is done using a leap frog scheme with the time step Δt chosen in such a way that the ratio $\Delta t/h$ is equal to the maximal value that ensures the stability. Perfectly matched layers are used to simulate a non bounded domain in all the boundaries.

Horizontal obstacle. In the first experiment we consider a plane horizontal crack

$$(x,z) \quad = \quad (5 + 2\sqrt{2}(2t-1), 5 - 2\sqrt{2})\text{mm}, \qquad t \in [0,1], \tag{17}$$

that we discretize using a uniform mesh of step $H = Rh$. The method converges and we obtain good results for reasonable values for the parameter R (in the interval $[0.75, 3]$). In the first column of figure 3 we show the results for $R = 1.2$. At the beginning, the wave is totally reflected by the boundary. When the wave front reach the tips of the crack, two scattered waves are created.

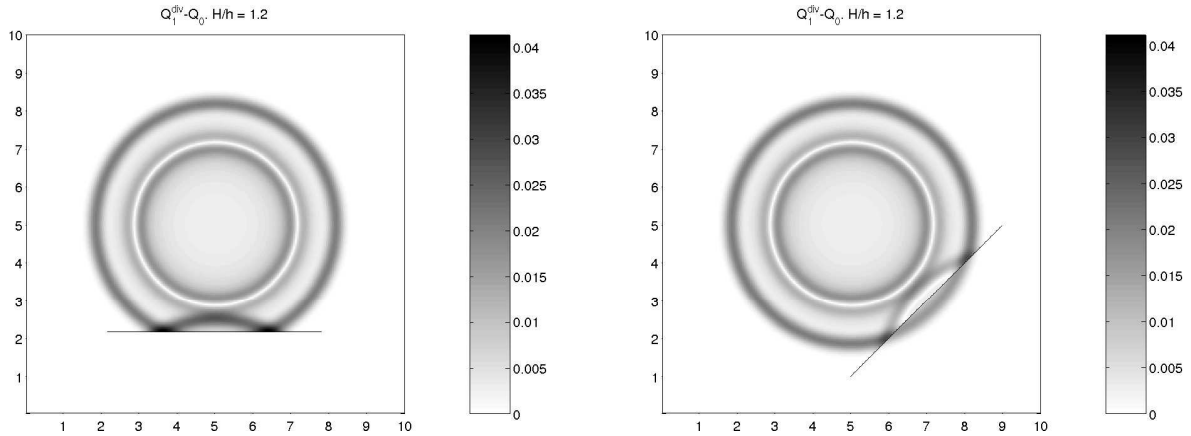

(a) $t = 2.6516506\ \mu$s (b) $t = 2.6516506\ \mu$s

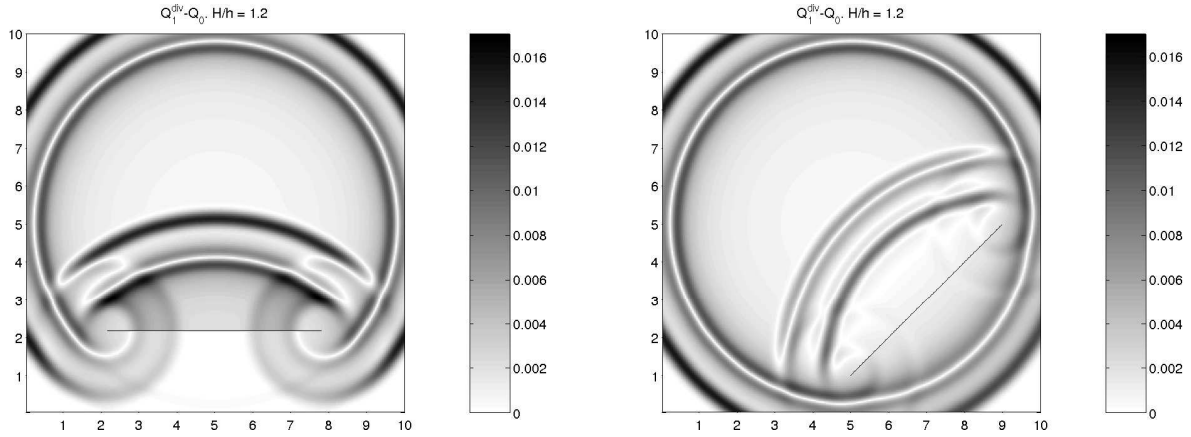

(c) $t = 5.3033012\ \mu$s (d) $t = 5.3033012\ \mu$s

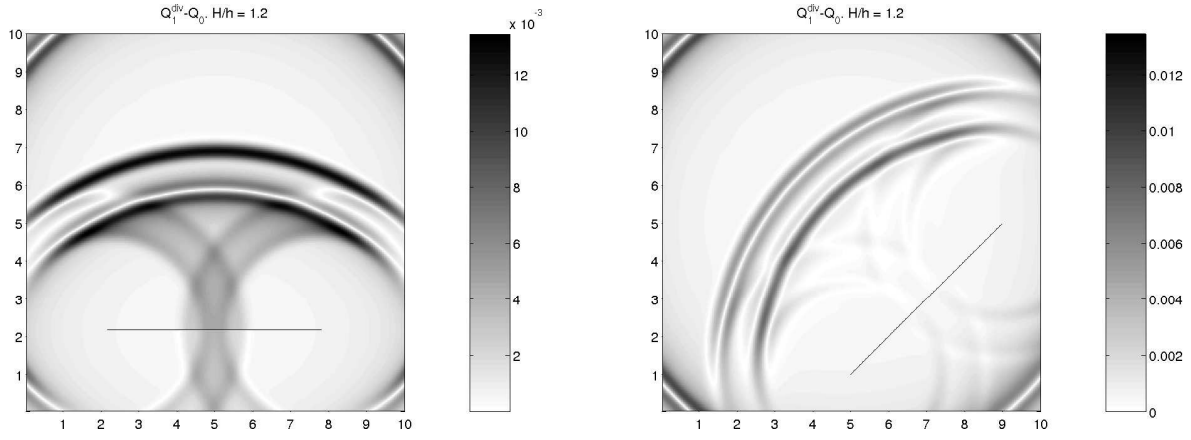

(e) $t = 7.0710683\ \mu$s (f) $t = 7.0710683\ \mu$s

Figure 3: $Q_1^{div} - Q_0$. Isotropic medium. $H/h = 1.2$

Diagonal obstacle. In the second experiment we treat a plane diagonal defect given by

$$(x,z) \quad = \quad (5+4t, 1+4t)\text{mm}, \qquad t \in [0,1], \tag{18}$$

that is, the same obstacle considered in the previous paragraph rotated by $\pi/4$ radians with respect to (x_c, z_c), the center of the initial condition. As the medium is isotropic, the solution of the continuous problem is also a rotation of the solution considering the horizontal crack.

We discretize the Lagrange multiplier using again a uniform mesh of step $H = Rh$ with several values for the parameter R. However, this time, the approximated solution does not seem to converge towards the physical solution (see for instance the second column of the figure 3 for $R = 1.2$). The incident wave is not completely reflected but also transmitted through the interface.

4 The modified element $Q_1^{div} - P_1^{disc}$

4.1 Presentation of the modified element

In section 3.1, we have conjectured that the difficulty of the convergence analysis comes from the fact that inclusion (16) is not satisfied. In order to avoid this problem we propose to modify the space M_h in such a way that

$$\text{div}\left(\underline{X_h}\right) \subset M_h, \tag{19}$$

which implies (16) and could simplify the analysis. That is why we have chosen to discretize the pressure in the space

$$M_h = M_h^1 \quad \text{with} \quad M_h^1 = \{q_h \in M \,/\, \forall K \in \mathcal{T}_h,\ q_h|_K \in P_1(K)\}\,. \tag{20}$$

Consequently, we will have three degrees of freedom per element on the unknown p_h as shown in figure 4. Since $M_h^0 \subset M_h^1$ we have obviously

$$\inf_{q_h \in M_h} \|p - q_h\|_\rho \leq \inf_{q_h^0 \in M_h^0} \left\|p - q_h^0\right\|_\rho,$$

so that the approximation properties (10) are still satisfied.

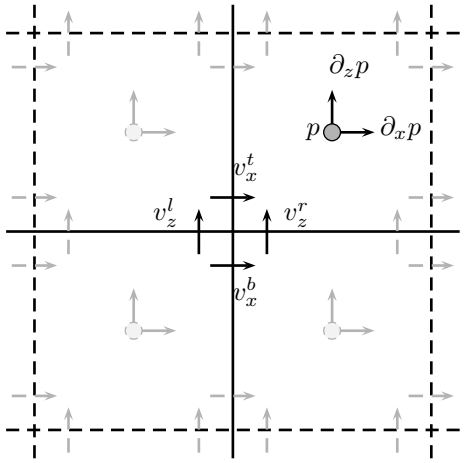

Figure 4: Degrees of freedom for the $Q_1^{div} \times P_1^{disc}$ mixed finite element.

Remark 2 *Assuming (19) and that the density is constant on each element we have that*

$$\mathbf{w}_h \in \underline{X_h} \implies q_h := \frac{1}{\rho}\text{div}(\mathbf{w}_h) \in M_h.$$

Introducing this particular test function in the second equation of (11) we obtain

$$\frac{d}{dt}\int_C p_h \text{div}(\mathbf{w}_h)dx - \int_C \frac{1}{\rho}\text{div}(\mathbf{v}_h)\text{div}(\mathbf{w}_h)dx = \int_C \frac{1}{\rho} f\,\text{div}(\mathbf{w}_h)dx.$$

Deriving with respect to time the first and third equations of (11) and using the last expression we deduce that our variational formulation implies the following second order formulation

$$\begin{cases} \text{Find } (\mathbf{v}_h(t), \tilde{\lambda}_H(t)) \in \underline{X_h} \times \mathcal{G}_H \text{ such that } \forall\ (\mathbf{w}_h, \mu_H) \in \underline{X_h} \times \mathcal{G}_H, \\ \dfrac{d^2}{dt^2}\displaystyle\int_C \mathbf{A}\mathbf{v}_h \cdot \mathbf{w}_h dx + \int_C \frac{1}{\rho}\text{div}(\mathbf{w}_h)\text{div}(\mathbf{v}_h)dx - \int_\Gamma \mathbf{w}_h \cdot \mathbf{n}\ \tilde{\lambda}_H d\gamma = \int_C -\frac{1}{\rho} f\,\text{div}(\mathbf{w}_h)dx, \\ \displaystyle\int_\Gamma \mathbf{v}_h \cdot \mathbf{n}\ \mu_H d\gamma = 0, \\ \mathbf{v}_h(t=0) = \mathbf{v}_{h,0}, \\ p_h(t=0) = p_{h,0}, \end{cases}$$

where $\tilde{\lambda}_H = \dfrac{\partial \lambda_H}{\partial t}$. *The nature of this problem is close to the ones analyzed in [13, 20].*

4.2 Some numerical illustrations of the fictitious domain method using the modified element

Let us now show some numerical illustrations of the behavior of the fictitious domain method with the new finite element space. The numerical experiments that we have considered are the same as in section 3.2 and will allow us to compare both finite elements.

Horizontal obstacle Once again we discretize the horizontal crack defined by (17) using a uniform mesh of step $H = Rh$. The results obtained with the new mixed finite element $Q_1^{div} - P_1^{disc}$ are similar to those given by the $Q_1^{div} - Q_0$ element. The method converges for reasonable values of the parameter R (in the interval $[0.75, 3]$). In the first column of the figure 5 we can see the results for $R = 1.2$.

Diagonal obstacle We now consider the diagonal crack defined by the expression (18). We recall that the continuous problem is a rotation of $\pi/4$ radians with respect to the point $(x_c, z_c) = (5, 5)$.

The Lagrange multiplier is again discretized using an uniform mesh of step $H = Rh$. Contrary to the results obtained with the element $Q_1^{div} - Q_0$, the ones given by the modified element $Q_1^{div} - P_1^{disc}$ converge towards the physical solution when choosing reasonable values for the ratio H/h. As we show in the second column of figure 5, this time the incident wave is almost completely reflected by the obstacle. The scattered waves created by the tips of the crack are well approached.

4.3 Dispersion analysis of the modified element

It is useful and classical to perform a dispersion analysis in order to specify the properties of a discrete scheme (in absence of obstacle) (e.g. [24, 9]). This consists in studying the behavior of discrete plane waves propagated with the scheme. We will show that two spurious modes that contaminate the discrete solution appear, for the modified element, because two new degrees of freedom per element were added for the pressure.

Assume that our computational domain $\Omega = \mathbb{R}^2$ is homogeneous and that we use a uniform mesh composed by squares of edge h. In this way, the degrees of freedom of the velocity field are placed at the vertices of the squares, that is, at the points $(x_i, z_j) = (ih, jh)$. We thus have,

$$(v_x^t)_{i,j}, \qquad (v_x^b)_{i,j}, \qquad (v_z^r)_{i,j}, \qquad (v_z^l)_{i,j}, \qquad (i,j) \in \mathbb{Z} \times \mathbb{Z}.$$

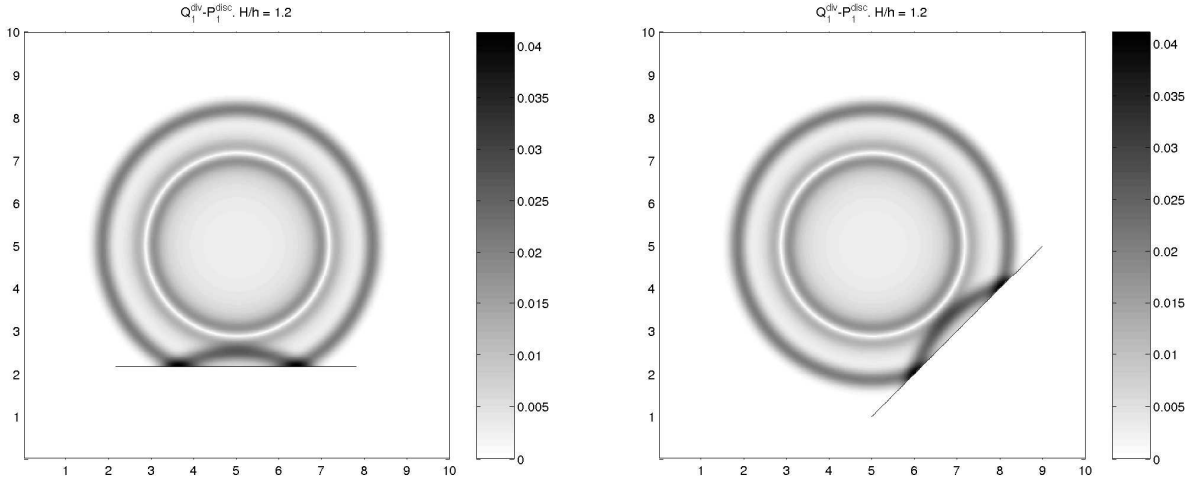

(a) $t = 2.6516506\ \mu$s (b) $t = 2.6516506\ \mu$s

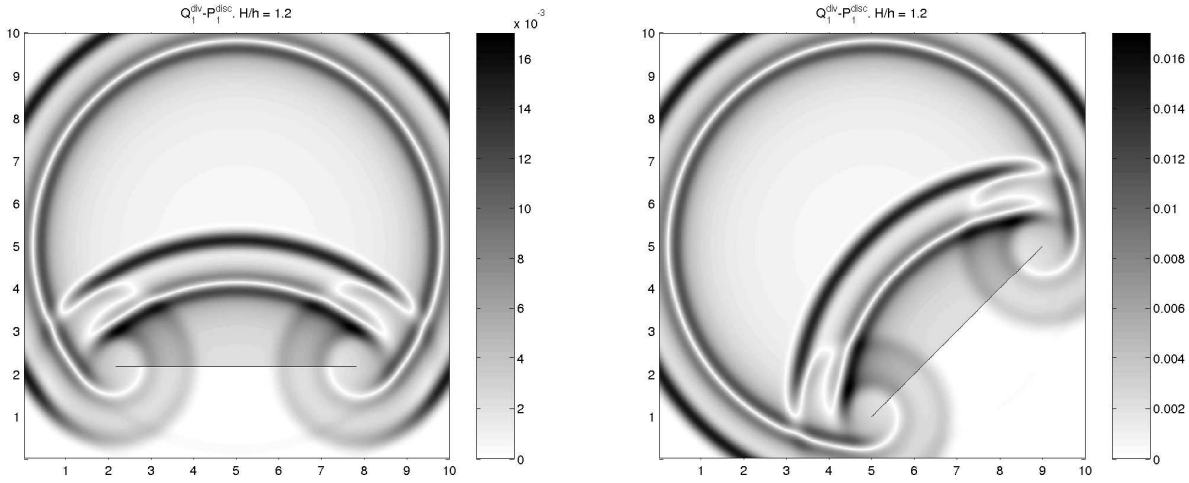

(c) $t = 5.3033012\ \mu$s (d) $t = 5.3033012\ \mu$s

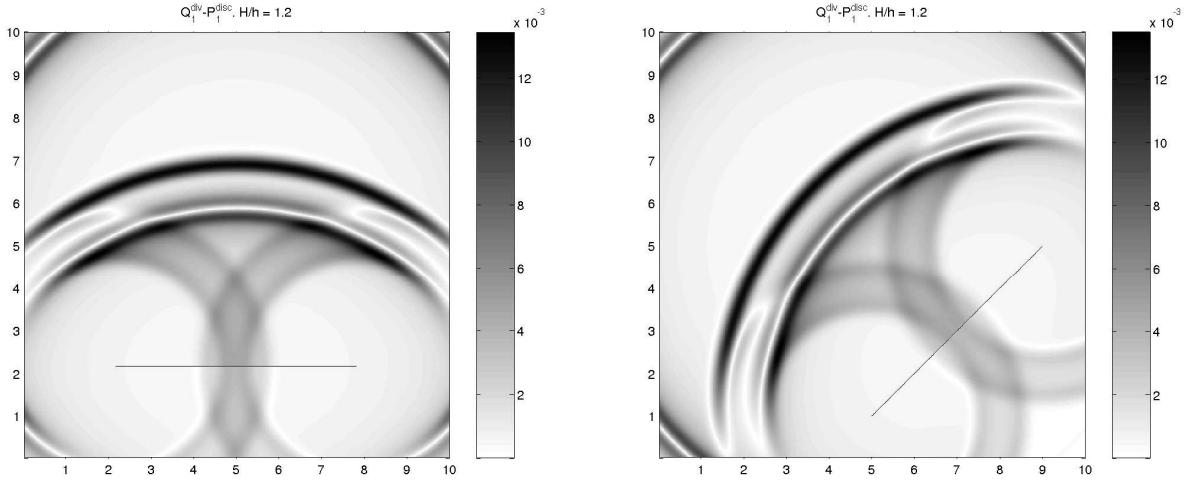

(e) $t = 7.0710683\ \mu$s (f) $t = 7.0710683\ \mu$s

Figure 5: $Q_1^{div} - P_1^{disc}$. Isotropic medium. $H/h = 1.2$

The degrees of freedom for the pressure are defined at the center of each element, that is, at the points $(x_{i+\frac{1}{2}}, z_{j+\frac{1}{2}}) = ((i+1/2)h, (j+1/2)h)$. The corresponding unknowns are denoted by,

$$(p)_{i+\frac{1}{2},j+\frac{1}{2}}, \qquad (\partial_x p)_{i+\frac{1}{2},j+\frac{1}{2}}, \qquad (\partial_z p)_{i+\frac{1}{2},j+\frac{1}{2}}, \qquad (i,j) \in \mathbb{Z} \times \mathbb{Z}.$$

The numerical scheme is thus given by,

$$\left| \begin{array}{rcl} \dfrac{\mathrm{d}}{\mathrm{d}t}(p)_{i+\frac{1}{2},j+\frac{1}{2}} & = & \dfrac{1}{2\rho h}\left\{(v_x^t)_{i+1,j} - (v_x^t)_{i,j} + (v_x^b)_{i+1,j+1} - (v_x^b)_{i,j+1}\right\} + \\ & & \dfrac{1}{2\rho h}\left\{(v_y^r)_{i,j+1} - (v_y^r)_{i,j} + (v_y^l)_{i+1,j+1} - (v_y^l)_{i+1,j}\right\}, \\ \dfrac{\mathrm{d}}{\mathrm{d}t}(\partial_x p)_{i+\frac{1}{2},j+\frac{1}{2}} & = & \dfrac{1}{\sqrt{12}\rho h}\left\{(v_y^l)_{i+1,j+1} - (v_y^l)_{i+1,j} - (v_y^r)_{i,j+1} + (v_y^r)_{i,j}\right\}, \\ \dfrac{\mathrm{d}}{\mathrm{d}t}(\partial_z p)_{i+\frac{1}{2},j+\frac{1}{2}} & = & \dfrac{1}{\sqrt{12}\rho h}\left\{(v_x^b)_{i+1,j+1} - (v_x^b)_{i,j+1} - (v_x^t)_{i+1,j} + (v_x^t)_{i,j}\right\}, \end{array} \right. \tag{21}$$

$$\left| \begin{bmatrix} \frac{A_{11}}{2} & 0 & \frac{A_{12}}{4} & \frac{A_{12}}{4} \\ 0 & \frac{A_{11}}{2} & \frac{A_{12}}{4} & \frac{A_{12}}{4} \\ \frac{A_{12}}{4} & \frac{A_{12}}{4} & \frac{A_{22}}{2} & 0 \\ \frac{A_{12}}{4} & \frac{A_{12}}{4} & 0 & \frac{A_{22}}{2} \end{bmatrix} \begin{bmatrix} \frac{\mathrm{d}}{\mathrm{d}t}(v_x^t)_{i,j} \\ \frac{\mathrm{d}}{\mathrm{d}t}(v_x^b)_{i,j} \\ \frac{\mathrm{d}}{\mathrm{d}t}(v_z^r)_{i,j} \\ \frac{\mathrm{d}}{\mathrm{d}t}(v_z^l)_{i,j} \end{bmatrix} = \begin{bmatrix} (B_1)_{i,j} \\ (B_2)_{i,j} \\ (B_3)_{i,j} \\ (B_4)_{i,j} \end{bmatrix}, \right. \tag{22}$$

where

$$\left| \begin{array}{rcl} (B_1)_{i,j} & = & \dfrac{1}{2h}\left((p)_{i+\frac{1}{2},j+\frac{1}{2}} - (p)_{i-\frac{1}{2},j+\frac{1}{2}}\right) - \dfrac{1}{\sqrt{12}h}\left((\partial_z p)_{i+\frac{1}{2},j+\frac{1}{2}} - (\partial_z p)_{i-\frac{1}{2},j+\frac{1}{2}}\right), \\ (B_2)_{i,j} & = & \dfrac{1}{2h}\left((p)_{i+\frac{1}{2},j-\frac{1}{2}} - (p)_{i-\frac{1}{2},j-\frac{1}{2}}\right) + \dfrac{1}{\sqrt{12}h}\left((\partial_z p)_{i+\frac{1}{2},j-\frac{1}{2}} - (\partial_z p)_{i-\frac{1}{2},j-\frac{1}{2}}\right), \\ (B_3)_{i,j} & = & \dfrac{1}{2h}\left((p)_{i+\frac{1}{2},j+\frac{1}{2}} - (p)_{i+\frac{1}{2},j-\frac{1}{2}}\right) - \dfrac{1}{\sqrt{12}h}\left((\partial_x p)_{i+\frac{1}{2},j+\frac{1}{2}} - (\partial_x p)_{i+\frac{1}{2},j-\frac{1}{2}}\right), \\ (B_4)_{i,j} & = & \dfrac{1}{2h}\left((p)_{i-\frac{1}{2},j+\frac{1}{2}} - (p)_{i-\frac{1}{2},j-\frac{1}{2}}\right) + \dfrac{1}{\sqrt{12}h}\left((\partial_x p)_{i-\frac{1}{2},j+\frac{1}{2}} - (\partial_x p)_{i-\frac{1}{2},j-\frac{1}{2}}\right). \end{array} \right.$$

We eliminate the unknowns associated to the velocity field using these last expressions to write a system on $(p, \partial_x p, \partial_z p)$. The next step of our analysis is to consider a plane wave solution for our problem at frequency ω and with wave vector $\mathbf{k} = (k_x, k_z)$, *i.e.*, we assume that

$$\left| \begin{array}{rcl} \begin{pmatrix} (p)_{i+\frac{1}{2},j+\frac{1}{2}} \\ (\partial_x p)_{i+\frac{1}{2},j+\frac{1}{2}} \\ (\partial_z p)_{i+\frac{1}{2},j+\frac{1}{2}} \end{pmatrix} & = & \mathbf{P} \exp\left[i\left(\omega t - (k_x x_{i+\frac{1}{2}} + k_z z_{j+\frac{1}{2}})\right)\right], \\ \mathbf{P} & = & [\,\mathbf{p}\,,\,\partial_{\mathbf{x}}\mathbf{p}\,,\,\partial_{\mathbf{z}}\mathbf{p}\,]^t, \end{array} \right. \tag{23}$$

Introducing this expression in the numerical scheme we note that the couple $\left(\omega^2, \mathbf{P}\right)$ must be solution of the following eigenvalue problem

$$\mathcal{K}\,\mathbf{P} = \frac{\omega^2}{k^2}\,\mathbf{P}, \quad \text{where } k = |\mathbf{k}|. \tag{24}$$

The hermitian matrix $\mathcal{K}$ is given by

$$
\begin{aligned}
(\mathcal{K}_h)_{11} &= \frac{1}{\rho(kh)^2}\left(2\mathcal{A}\sin^2\left(\frac{k_xh}{2}\right)+2\mathcal{C}\sin^2\left(\frac{k_zh}{2}\right)+2\mathcal{E}\sin(k_xh)\sin(k_zh)+\right.\\
&\qquad\left.2\mathcal{B}\cos(k_zh)\sin^2\left(\frac{k_xh}{2}\right)+2\mathcal{D}\cos(k_xh)\sin^2\left(\frac{k_zh}{2}\right)\right),\\
(\mathcal{K}_h)_{12} &= \frac{-1}{\rho(kh)^2}\left(\frac{2I\mathcal{E}}{\sqrt{3}}\sin(k_zh)\sin^2\left(\frac{k_xh}{2}\right)+\frac{2I\mathcal{D}}{\sqrt{3}}\sin(k_xh)\sin^2\left(\frac{k_zh}{2}\right)\right),\\
(\mathcal{K}_h)_{13} &= \frac{-1}{\rho(kh)^2}\left(\frac{2I\mathcal{E}}{\sqrt{3}}\sin(k_xh)\sin^2\left(\frac{k_zh}{2}\right)-\frac{2I\mathcal{B}}{\sqrt{3}}\sin(k_zh)\sin^2\left(\frac{k_xh}{2}\right)\right),\\
(\mathcal{K}_h)_{22} &= \frac{1}{\rho(kh)^2}\left(\frac{2\mathcal{C}}{3}\sin^2\left(\frac{k_zh}{2}\right)-\frac{2\mathcal{D}}{3}\cos(k_xh)\sin^2\left(\frac{k_zh}{2}\right)\right),\\
(\mathcal{K}_h)_{23} &= \frac{4\mathcal{E}}{3\rho(kh)^2}\sin^2\left(\frac{k_xh}{2}\right)\sin^2\left(\frac{k_zh}{2}\right),\\
(\mathcal{K}_h)_{33} &= \frac{1}{\rho(kh)^2}\left(\frac{2\mathcal{A}}{3}\sin^2\left(\frac{k_xh}{2}\right)-\frac{2\mathcal{B}}{3}\cos(k_zh)\sin^2\left(\frac{k_xh}{2}\right)\right),
\end{aligned}
$$

where

$$
\left|\begin{array}{lllllll}
\mathcal{A} &=& \dfrac{2C_{11}C_{22}-C_{12}^2}{C_{22}}, & \mathcal{C} &=& \dfrac{2C_{11}C_{22}-C_{12}^2}{C_{11}},\\
\mathcal{B} &=& \dfrac{C_{12}^2}{C_{22}}, & \mathcal{D} &=& \dfrac{C_{12}^2}{C_{11}}, \qquad \mathcal{E} = C_{12}.
\end{array}\right. \tag{25}
$$

and the tensor $\mathbf{C}=(C_{ij})$ denotes the inverse of the tensor $\mathbf{A}$, $\mathbf{C}=\mathbf{A}^{-1}$. Since the matrix $\mathcal{K}$ is hermitian, there are three real eigenvalues with three orthogonal eigenvectors. Performing a Taylor expansion we obtain the following results. For the first couple denoted $(\omega_{phys}^2,\mathbf{P}_{phys})$ we have,

$$
\left|\begin{array}{lll}
c_{h,phys} = \dfrac{\omega_{phys}}{k} &=& \sqrt{\dfrac{\cos^2(\theta)C_{11}+\sin^2(\theta)C_{22}+2C_{12}\sin(\theta)\cos(\theta)}{\rho}}+\mathcal{O}(kh)^2,\\
\mathbf{V_{phys}} &=& [\,1\,,\,0\,,\,0\,]^t \;+\; \mathcal{O}(kh).
\end{array}\right.
$$

The phase velocity of the physical numerical wave is a second order approximation of the phase velocity of the continuous wave. The other two solutions are spurious modes produced by the introduction of the additional degrees of freedom and are given by,

$$
\left|\begin{array}{lll}
c_{h,spur1} = \dfrac{\omega_{spur1}}{k} &=& \sqrt{\dfrac{\sin^2(\theta)\left(C_{11}C_{22}-C_{12}^2\right)}{3\,\rho\,C_{11}}}+\mathcal{O}(kh)^2,\\
\mathbf{V_{spur1}} &=& [\,0\,,\,1\,,\,0\,]^t \;+\; \mathcal{O}(kh),
\end{array}\right.
$$

$$
\left|\begin{array}{lll}
c_{h,spur2} = \dfrac{\omega_{spur2}}{k} &=& \sqrt{\dfrac{\cos^2(\theta)\left(C_{11}C_{22}-C_{12}^2\right)}{3\,\rho\,C_{22}}}+\mathcal{O}(kh)^2,\\
\mathbf{V_{spur2}} &=& [\,0\,,\,0\,,\,1\,]^t \;+\; \mathcal{O}(kh).
\end{array}\right.
$$

4.4 Damping of the spurious modes

As we have seen in the previous section, the modified element gives rise to some spurious modes. In this section we propose a way to damp the amplitude of these modes (without damping the "physical part"), so that they do not perturb too much the approximate solution.

The modified space M_h^1 can be decomposed as

$$M_h = M_h^0 \oplus M_h^r, \tag{26}$$

where M_h^0 is the space of piecewise constants and M_h^r is its orthogonal complement (for the L^2 scalar product). The space M_h^r is composed of P_1 discontinuous functions with vanishing mean value per element.

From the dispersion analysis, we observe that the main components of the spurious modes (the O(1) part) belong to M_h^r. In order to damp this main part, we introduce the L^2 orthogonal projection on M_h^r, that we denote by $P_{M_h^r}$, defined for any $p \in M_h$ as,

$$P_{M_h^r}(p) \in M_h^r \quad \text{and} \quad (P_{M_h^r}(p), q_h) = (p, q_h), \quad \forall q_h \in M_h^r.$$

The approximate problem with damping consists in finding $(p_h, \mathbf{v}_h) \in M_h \times \underline{X_h}$ such that

$$\left\{ \begin{array}{l} \dfrac{d}{dt} a(\mathbf{v}_h, \mathbf{w}_h) + b(\mathbf{w}_h, p_h) - < \mathbf{w}_h \cdot n, \lambda_H >_\Gamma = 0, \quad \forall \mathbf{w}_h \in \underline{X_h}, \\ \dfrac{d}{dt}(p_h, q_h)_\rho + (P_{M_h^r}(p_h), q_h)_\beta - b(\mathbf{v}_h, q_h) = (f, q_h), \quad \forall q_h \in M_h, \\ < \mathbf{v}_h \cdot n, \mu_H >_\Gamma = 0, \quad \forall \mu_H \in \mathcal{G}_H. \end{array} \right. \tag{27}$$

In this system β represents a damping parameter, which is chosen as a positive constant in the applications. The case $\beta = 0$ gives back the non-damped problem, while a strictly positive β corresponds to a dissipative problem. From the numerical point of view, it remains to define a procedure in order to choose this parameter in an appropriate way.

5 Convergence analysis

In this section we show the convergence of the fictitious domain method using the modified element with damping. The proof of convergence is composed of two main steps. One step consists in relating, using energy techniques, error estimates for the evolution problem in terms of the difference between the exact solution and its elliptic projection (that has to be cleverly defined). The second step amounts to analyzing the elliptic projection error and we will start with this point.

5.1 Elliptic projection error

We define the elliptic projection operator in the following way:

$$(\mathbf{v}, p, \lambda) \in \underline{X} \times M \times \mathcal{G} \to \Pi_h(\mathbf{v}, p, \lambda) = (\widehat{\mathbf{v}}_h, \widehat{p}_h, \widehat{\lambda}_H) \in \underline{X_h} \times M_h \times \mathcal{G}_H,$$

where $(\widehat{\mathbf{v}}_h, \widehat{p}_h, \widehat{\lambda}_H) \in \underline{X_h} \times M_h \times \mathcal{G}_H$ is solution of

$$\left| \begin{array}{l} (\widehat{p}_h - p, q_h) - b(\widehat{\mathbf{v}}_h - \mathbf{v}, q_h) = 0, \quad \forall q_h \in M_h, \\ a(\widehat{\mathbf{v}}_h - \mathbf{v}, \mathbf{w}_h) + b(\mathbf{w}_h, \widehat{p}_h - p) - < \mathbf{w}_h \cdot \mathbf{n}, \widehat{\lambda}_H - \lambda >_\Gamma = 0, \quad \forall \mathbf{w}_h \in \underline{X_h}, \\ < (\widehat{\mathbf{v}}_h - \mathbf{v}) \cdot \mathbf{n}, \mu_H >_\Gamma = 0, \quad \forall \mu_H \in \mathcal{G}_H. \end{array} \right. \tag{28}$$

It is easy to show that this problem is equivalent to define first the couple $(\widehat{\mathbf{v}}_h, \widehat{\lambda}_H) \in \underline{X_h} \times \mathcal{G}_H$ satisfying

$$\left\{ \begin{array}{rcl} a(\widehat{\mathbf{v}}_h - \mathbf{v}, \mathbf{w}_h) + (\mathrm{div}(\widehat{\mathbf{v}}_h - \mathbf{v}), \mathrm{div}\mathbf{w}_h) & - & < \mathbf{w}_h \cdot \mathbf{n}, \lambda - \widehat{\lambda}_H >_\Gamma \;=\; 0, \quad \forall \mathbf{w}_h \in \underline{X_h}, \\ & & < (\mathbf{v} - \widehat{\mathbf{v}}_h) \cdot \mathbf{n}, \mu_H >_\Gamma \;=\; 0, \quad \forall \mu_H \in \mathcal{G}_H, \end{array} \right. \tag{29}$$

and then $\widehat{p}_h \in M_h$ satisfying

$$(\widehat{p}_h - p, q_h) = b(\widehat{\mathbf{v}}_h - \mathbf{v}, q_h), \quad \forall q_h \in M_h. \tag{30}$$

This follows from the fact that div $\underline{X_h} \subset M_h$, so that we can choose $q_h = \mathrm{div}\, \mathbf{w}_h$. It is well known that the convergence of $(\widehat{\mathbf{v}}_h, \widehat{\lambda}_H)$ to $(\mathbf{v}, \lambda)$ is related to the uniform discrete inf-sup condition,

$$\left| \begin{array}{l} \exists C > 0 \text{ independent of } h \text{ such that} \\ \\ \forall \mu_H \in \mathcal{G}_H, \exists \mathbf{w}_h \in \underline{X_h}, \; < \mathbf{w}_h \cdot \mathbf{n}, \mu_H >_\Gamma \geq C \left\| \mathbf{w}_h \right\|_{\underline{X}} \left\| \mu_H \right\|_{\mathcal{G}}. \end{array} \right. \tag{31}$$

Theorem 5.1 *If assumption (13) is satisfied, then there exists a constant $\alpha > 0$ such that if $H \geq \alpha h$, the uniform discrete inf-sup condition (31) is satisfied for the couple of spaces $(\underline{X_h}, \mathcal{G}_H)$.*

Proof. The result has been shown in [20] for the couple of spaces $(\underline{X_h}^{RT}, \mathcal{G}_H)$. The space $\underline{X_h}$ considered here clearly contains $\underline{X_h}^{RT}$ (cf. [4]), which shows that the inf-sup condition is still true for the couple $(\underline{X_h}, \mathcal{G}_H)$. □

Once the inf-sup condition is satisfied, there is no difficulty in applying the classical Babushka-Brezzi [8] theory and we obtain the elliptic projection estimates,

Theorem 5.2 *We assume that $H \geq \alpha h$ where α is the constant given in theorem 5.1. The problem (28) has a unique solution $(\widehat{p}_h, \widehat{\mathbf{v}}_h, \widehat{\lambda}_H) \in M_h \times \underline{X_h} \times \mathcal{G}_H$ which satisfies*

$$\left\| \mathbf{v} - \widehat{\mathbf{v}}_h \right\|_{\underline{X}} + \left\| \lambda - \widehat{\lambda}_H \right\|_{\mathcal{G}} \leq C \left(\inf_{\mathbf{w}_h \in \underline{X_h}} \left\| \mathbf{v} - \mathbf{w}_h \right\|_{\underline{X}} + \inf_{\mu_H \in \mathcal{G}_H} \left\| \lambda - \mu_H \right\|_{\mathcal{G}} \right), \tag{32}$$

$$\left\| p - \widehat{p}_h \right\|_M \leq C \left(\inf_{q_h \in M_h} \left\| p - q_h \right\|_M + \inf_{\mathbf{w}_h \in \underline{X_h}} \left\| \mathbf{v} - \mathbf{w}_h \right\|_{\underline{X}} + \inf_{\mu_H \in \mathcal{G}_H} \left\| \lambda - \mu_H \right\|_{\mathcal{G}} \right). \tag{33}$$

Proof. The error estimates for $(\mathbf{v} - \widehat{\mathbf{v}}_h, \lambda - \widehat{\lambda}_H)$ follow from the classical theory [8]. For $\widehat{p}_h$, we use (30) which implies that

$$\left\| \widehat{p}_h - q_h \right\|_M \leq \left\| p - q_h \right\|_M + \left\| \mathrm{div}\, (\widehat{\mathbf{v}}_h - \mathbf{v}) \right\|, \quad \forall\, q_h \in M_h,$$

and then

$$\left\| \widehat{p}_h - p \right\|_M \leq 2 \inf_{q_h \in M_h} \left\| p - q_h \right\|_M + \left\| \widehat{\mathbf{v}}_h - \mathbf{v} \right\|_{\underline{X}}.$$

□

The following theorem shows that only the projection of the pressure on M_h^0 tends to p, since the other part tends to zero.

Theorem 5.3 *We assume that $H \geq \alpha h$ where α is the constant given in theorem 5.1. If $(\widehat{p}_h^0, \widehat{p}_h^r) = (P_{M_h^0}(p_h), P_{M_h^r}(p_h)) \in M_h^0 \times M_h^r$ denote the orthogonal projections of p_h on M_h^0 and M_h^r, we have:*

$$\left\| \widehat{p}_h^0 - p \right\|_M + \left\| \widehat{p}_h^r \right\|_M \leq C(\inf_{\mathbf{w}_h \in \underline{X_h}} \left\| \mathbf{v} - \mathbf{w}_h \right\|_{\underline{X}} + \inf_{\mu_H \in \mathcal{G}_H} \left\| \lambda - \mu_H \right\|_{\mathcal{G}} + \inf_{q_h^0 \in M_h^0} \left\| p - q_h^0 \right\|_M). \tag{34}$$

Proof. Using equation (30) for $q_h^0 \in M_h^0$, all the terms in M_h^r disappear,

$$(\widehat{p}_h^0 - p, q_h^0) = b(\widehat{\mathbf{v}}_h - \mathbf{v}, q_h^0), \quad \forall q_h^0.$$

With the same arguments as previously we obtain,

$$\left\|\widehat{p}_h^0 - p\right\|_M \leq C(\|\text{div}\,(\widehat{\mathbf{v}}_h - \mathbf{v})\| + \inf_{q_h^0 \in M_h^0} \left\|p - q_h^0\right\|_M).$$

Since $\widehat{p}_h^r = \widehat{p}_h - p + p - \widehat{p}_h^0$, it suffices to combine both estimates (33) and the first estimate of (34) to obtain the estimate on $\widehat{p}_h^r$. □

Remark 3 *The elliptic projection of time dependent functions $(\mathbf{v}, p, \lambda)$ depends also on time and it is easy to check that if*

$$(\mathbf{v}, p, \lambda) \ \in \ C^k\left([0,T]; \underline{X} \times M \times \mathcal{G}\right),$$

then

$$\Pi_h(\mathbf{v}, p, \lambda) \ \in \ C^k\left([0,T]; \underline{X}_h \times M_h \times \mathcal{G}_H\right),$$

and

$$\frac{\partial^k}{\partial t^k}\Pi_h(\mathbf{v}, p, \lambda) \ = \ \Pi_h\left(\frac{\partial^k \mathbf{v}}{\partial t^k}, \frac{\partial^k p}{\partial t^k}, \frac{\partial^k \lambda}{\partial t^k}\right).$$

We will also need in the following error estimates on the time derivative of the elliptic projection,

Corollaire 5.1 *We assume that $H \geq \alpha h$ where α is the constant given in theorem 5.1 and that $(\mathbf{v}, p, \lambda)$ depend on time t and*

$$(\mathbf{v}, p, \lambda) \in \mathcal{C}^k\left([0,T]; \underline{X} \times M \times \mathcal{G}\right).$$

Then

$$\|\partial_t^k(\widehat{\mathbf{v}}_h - \mathbf{v})\|_{\underline{X}} + \|\partial_t^k(\widehat{\lambda}_H - \lambda)\|_{\mathcal{G}} \ \leq \ \mathcal{C}\left(\inf_{\mathbf{w}_h \in \underline{X}_h} \|\mathbf{w}_h - \partial_t^k \mathbf{v}\|_{\underline{X}} + \inf_{\mu_H \in \mathcal{G}_H} \|\mu_H - \partial_t^k \lambda\|_{\mathcal{G}}\right), \tag{35}$$

$$\begin{aligned} \|\partial_t^k\left(\widehat{p}_h - p\right)\|_M \ \leq \ \mathcal{C}\Bigg(&\inf_{\mathbf{w}_h \in \underline{X}_h} \|\mathbf{w}_h - \partial_t^k \mathbf{v}\|_{\underline{X}} + \\ &\inf_{q_h \in M_h} \|q_h - \partial_t^k p\|_M + \inf_{\mu_H \in \mathcal{G}_H} \|\mu_H - \partial_t^k \lambda\|_{\mathcal{G}}\Bigg), \end{aligned} \tag{36}$$

$$\begin{aligned} \|P_{M_h^0}(\partial_t^k \widehat{p}_h) - \partial_t^k p\|_M + \|P_{M_h^r}(\partial_t^k \widehat{p}_h)\|_M \ \leq \ \mathcal{C}\Bigg(&\inf_{\mathbf{w}_h \in \underline{X}_h} \|\mathbf{w}_h - \partial_t^k \mathbf{v}\|_{\underline{X}} + \\ &\inf_{q_h^0 \in M_h^0} \|q_h^0 - \partial_t^k p\|_M + \inf_{\mu_H \in \mathcal{G}_H} \|\mu_H - \partial_t^k \lambda\|_{\mathcal{G}}\Bigg). \end{aligned} \tag{37}$$

Finally, classical approximation properties for finite elements give estimates with respect to h, for more regularity, *i.e.*, for $\varepsilon > 0$:

$$\begin{aligned} \inf_{\mathbf{w}_h \in \underline{X_h}} \|\mathbf{v} - \mathbf{w}_h\|_{\underline{X}} &\leq Ch^{1/2-\varepsilon} \|\mathbf{v}\|_{H^{\frac{1}{2}-\varepsilon}_{div}}, && \forall \mathbf{v} \in H^{\frac{1}{2}-\varepsilon}(\text{div}, C), \\ \inf_{q_h \in M_h} \|p - q_h\|_M &\leq Ch^{1/2-\varepsilon} \|p\|_{H^{\frac{1}{2}-\varepsilon}}, && \forall p \in H^{\frac{1}{2}-\varepsilon}(C), \\ \inf_{\mu_H \in \mathcal{G}_H} \|\lambda - \mu_H\|_{\mathcal{G}} &\leq CH^{1/2-\varepsilon} \|\lambda\|_{H^{1-\varepsilon}(\Gamma)}, && \forall \lambda \in H^{1-\varepsilon}(\Gamma). \end{aligned} \tag{38}$$

and this finally implies the following error estimates with respect to h.

Corollaire 5.2 *Assume that*

$$(\mathbf{v}, p, \lambda) \in \mathcal{C}^k\left([0,T]; H^{\frac{1}{2}-\varepsilon}(\mathrm{div}, C) \times H^{\frac{1}{2}-\varepsilon}(C) \times H^{1-\varepsilon}(\Gamma)\right), \quad \varepsilon > 0$$

and that $H \geq \alpha h$ where α is the constant given in theorem 5.1. Then we have the estimates

$$\left| \begin{array}{l} \|\partial_t^k(\widehat{\mathbf{v}}_h - \mathbf{v})\|_{\underline{X}} + \|\partial_t^k(\widehat{\lambda}_H - \lambda)\|_{\mathcal{G}} \leq \\ \qquad \mathcal{C}\left(h^{\frac{1}{2}-\varepsilon}\|\partial_t^k \mathbf{v}\|_{H^{\frac{1}{2}-\varepsilon}_{div}} + H^{\frac{1}{2}-\varepsilon}\|\partial_t^k \lambda\|_{H^{1-\varepsilon}(\Gamma)}\right), \end{array} \right. \tag{39}$$

$$\left| \begin{array}{l} \|P_{M_h^0}(\partial_t^k \widehat{p}_h) - \partial_t^k p\|_M + \|P_{M_h^r}(\partial_t^k \widehat{p}_h)\|_M \leq \\ \qquad \mathcal{C}\left(h^{\frac{1}{2}-\varepsilon}\left(\|\partial_t^k \mathbf{v}\|_{H^{\frac{1}{2}-\varepsilon}_{div}(C)} + \|\partial_t^k p\|_{H^{\frac{1}{2}-\varepsilon}(C)}\right) + H^{\frac{1}{2}-\varepsilon}\|\partial_t^k \lambda\|_{H^{1-\varepsilon}(\Gamma)}\right). \end{array} \right. \tag{40}$$

5.2 Error estimates

The error estimates for the evolution problem are then quite standard. They follow from energy estimates. We define the discrete energy of the error as

$$\mathcal{E}_h = \|\widehat{p}_h - p_h\|_\rho^2 + a(\widehat{\mathbf{v}}_h - \mathbf{v}_h, \widehat{\mathbf{v}}_h - \mathbf{v}_h). \tag{41}$$

We first prove the energy identity:

Theorem 5.4 *The discrete energy of the error satisfies the identity,*

$$\frac{d\mathcal{E}_h}{dt} + \int_C \beta|\widehat{p}_h^r - p_h^r|^2 = F, \tag{42}$$

where

$$\begin{array}{rcl} F & = & \dfrac{d}{dt}\left((\widehat{p}_h - p, \widehat{p}_h - p_h)_\rho + a(\widehat{\mathbf{v}}_h - \mathbf{v}, \widehat{\mathbf{v}}_h - \mathbf{v}_h)\right) \\ & & -(\widehat{p}_h - p, \widehat{p}_h - p_h)_\rho - a(\widehat{\mathbf{v}}_h - \mathbf{v}, \widehat{\mathbf{v}}_h - \mathbf{v}_h) + \displaystyle\int_C \beta \widehat{p}_h^r(\widehat{p}_h^r - p_h^r). \end{array} \tag{43}$$

Proof. The difference between the continuous problem (5) and the discrete one (27) gives a problem satisfied by the error

$$(\mathbf{v}_h - \mathbf{v}, p_h - p, \lambda_H - \lambda) = (\widehat{\mathbf{v}}_h - \mathbf{v}, \widehat{p}_h - p, \widehat{\lambda}_H - \lambda) + (\mathbf{v}_h - \widehat{\mathbf{v}}_h, p_h - \widehat{p}_h, \lambda_H - \widehat{\lambda}_H).$$

Using the definition of the elliptic projection operator, all the embarrassing terms disappear (the terms which would give rise to difficulty in obtaining the energy estimate, essentially those not equivalent to L^2 norms). It remains; $\forall (q_h, \mathbf{w}_h, \mu_H) \in M_h \times \underline{X_h} \times \mathcal{G}_H$:

$$\left\{ \begin{array}{l} \dfrac{d}{dt}(\widehat{p}_h - p_h, q_h)_\rho - (\beta p_h^r, q_h) - b((\widehat{\mathbf{v}}_h - \mathbf{v}_h), q_h) = \dfrac{d}{dt}(\widehat{p}_h - p, q_h)_\rho - (\widehat{p}_h - p, q_h)_\rho, \\ \dfrac{d}{dt}a(\widehat{\mathbf{v}}_h - \mathbf{v}_h, \mathbf{w}_h) + b(\mathbf{w}_h, \widehat{p}_h - p_h) - < \widetilde{\mathbf{v}}_h \cdot \mathbf{n}, \widehat{\lambda}_H - \lambda_H >_\Gamma = \\ \qquad\qquad = \dfrac{d}{dt}a(\widehat{\mathbf{v}}_h - \mathbf{v}, \mathbf{w}_h) - a(\widehat{\mathbf{v}}_h - \mathbf{v}, \mathbf{w}_h), \\ < (\widehat{\mathbf{v}}_h - \mathbf{v}_h) \cdot \mathbf{n}, \mu_H >_\Gamma = 0. \end{array} \right.$$

For $q_h = \widehat{p}_h - p_h$ and $\mathbf{w}_h = \widehat{\mathbf{v}}_h - \mathbf{v}_h$ we obtain

$$\left|\begin{array}{l} \dfrac{d}{dt}\|\widehat{p}_h - p_h\|_\rho^2 - (p_h^r, \widehat{p}_h - p_h)_\beta - b((\widehat{\mathbf{v}}_h - \mathbf{v}_h), \widehat{p}_h - p_h) = \\ \qquad\qquad = \dfrac{d}{dt}(\widehat{p}_h - p, \widehat{p}_h - p_h)_\rho - (\widehat{p}_h - p, \widehat{p}_h - p_h)_\rho, \\ \dfrac{d}{dt}a(\widehat{\mathbf{v}}_h - \mathbf{v}_h, \widehat{\mathbf{v}}_h - \mathbf{v}_h) + b((\widehat{\mathbf{v}}_h - \mathbf{v}_h), \widehat{p}_h - p_h) - < (\widehat{\mathbf{v}}_h - \mathbf{v}_h)\cdot\mathbf{n}, \widehat{\lambda}_H - \lambda_H >_\Gamma = \\ \qquad\qquad = \dfrac{d}{dt}a(\widehat{\mathbf{v}}_h - \mathbf{v}, \widehat{\mathbf{v}}_h - \mathbf{v}_h) - a(\widehat{\mathbf{v}}_h - \mathbf{v}, \widehat{\mathbf{v}}_h - \mathbf{v}_h), \\ < (\widehat{\mathbf{v}}_h - \mathbf{v}_h)\cdot\mathbf{n}, \mu_H >_\Gamma = 0, \quad \forall \mu_H \in \mathcal{G}_H. \end{array}\right.$$

Adding the first two equations and using the third one gives (42). □

The following proposition gives a bound of the discrete energy of the error in terms of the elliptic projection error.

Proposition 5.1 *The discrete energy of the error satisfies the following estimate:*

$$\left|\begin{array}{l} \sup\limits_{t'\le T} \mathcal{E}_h^{\frac{1}{2}}(t') \le \mathcal{C}\,\mathcal{E}_h^{\frac{1}{2}}(0) + \mathcal{C}\displaystyle\int_0^T \left(\|\partial_t(\widehat{p}_h - p)\|_M + \|\partial_t(\widehat{\mathbf{v}}_h - \mathbf{v})\|_{\underline{L^2}(C)} + \right. \\ \qquad\qquad \left. \|\widehat{p}_h - p\|_M + \|\widehat{\mathbf{v}}_h - \mathbf{v}\|_{\underline{L^2}(C)}\right) ds + \mathcal{C}\left[\displaystyle\int_0^T \|\sqrt{\beta}P_{M_h^r}(\widehat{p}_h)\|_M^2 ds\right]^{\frac{1}{2}}, \end{array}\right. \tag{44}$$

where $\mathcal{C}$ is a constant independent of h and β.

Proof. The proof is based on equality (42). Due to Young's inequality, the last term in (43) can be bounded by:

$$\int_C \left|\beta P_{M_h^r}(\widehat{p}_h) P_{M_h^r}(\widehat{p}_h - p_h)\right| \mathrm{d}x \le \int_C \beta \left|P_{M_h^r}(\widehat{p}_h - p_h)\right|^2 \mathrm{d}x + \int_C \frac{\beta}{4}\left|P_{M_h^r}(\widehat{p}_h)\right|^2 \mathrm{d}x.$$

Simple computations then give

$$\begin{aligned} \frac{\mathrm{d}}{\mathrm{d}t}\mathcal{E}_h(t) &\le \mathcal{C}\|\widehat{p}_h - p_h\|_M \left(\|\partial_t(\widehat{p}_h - p)\|_M + \|\widehat{p}_h - p\|_M\right) + \\ &\quad \mathcal{C}\|\widehat{\mathbf{v}}_h - \mathbf{v}_h\|_{\underline{L^2}(C)} \left(\|\partial_t(\widehat{\mathbf{v}}_h - \mathbf{v})\|_{\underline{L^2}(C)} + \|\widehat{\mathbf{v}}_h - \mathbf{v}\|_{\underline{L^2}(C)}\right) + \frac{1}{4}\|\sqrt{\beta}P_{M_h^r}(\widehat{p}_h)\|_M^2 \\ &\le \mathcal{C}\mathcal{E}_h^{\frac{1}{2}}(t)\left(\|\partial_t(\widehat{p}_h - p)\|_M + \|\widehat{p}_h - p\|_M + \|\partial_t(\widehat{\mathbf{v}}_h - \mathbf{v})\|_{\underline{L^2}(C)} + \|\widehat{\mathbf{v}}_h - \mathbf{v}\|_{\underline{L^2}(C)}\right) \\ &\quad + \frac{1}{4}\|\sqrt{\beta}P_{M_h^r}(\widehat{p}_h)\|_M^2 \end{aligned}$$

Integrating in time, we obtain ($\forall\, t \le T$)

$$\begin{aligned} \mathcal{E}_h(t) &\le \mathcal{E}_h(0) + \mathcal{C}\sup_{t'\le T}\mathcal{E}_h^{\frac{1}{2}}(t')\int_0^T \left(\|\partial_t(\widehat{p}_h - p)\|_M + \|\partial_t(\widehat{\mathbf{v}}_h - \mathbf{v})\|_{\underline{L^2}(C)}\right. \\ &\quad \left. + \|\widehat{p}_h - p\|_M + \|\widehat{\mathbf{v}}_h - \mathbf{v}\|_{\underline{L^2}(C)}\right) \mathrm{d}s + \frac{1}{4}\int_0^T \|\sqrt{\beta}P_{M_h^r}(\widehat{p}_h)\|_M^2 \mathrm{d}s. \end{aligned}$$

We then take the maximum on $t \leq T$ and apply Young's inequality to the first integral term :

$$\begin{aligned}\sup_{t'\leq T} \mathcal{E}_h(t') \;\; &\leq \;\; \mathcal{C}\,\mathcal{E}_h(0) + \mathcal{C}\left[\int_0^T \left(\|\partial_t(\widehat{p}_h - p)\|_M + \|\partial_t(\widehat{\mathbf{v}}_h - \mathbf{v})\|_{\underline{L^2}(C)}\right.\right. \\ &\left.\left. + \|\widehat{p}_h - p\|_M + \|\widehat{\mathbf{v}}_h - \mathbf{v}\|_{\underline{L^2}(C)}\right) \mathrm{d}s\right]^2 + \mathcal{C}\int_0^T \|\sqrt{\beta} P_{M_h^r}(\widehat{p}_h)\|_M^2 \mathrm{d}s,\end{aligned}$$

which easily implies (44). □

We can now give error estimates:

Theorem 5.5 *Let $f \in C^0([0,T], M)$, $\mathbf{v}_0 \in \underline{X}$, $p_0 \in M$ satisfying (3) and $(\mathbf{v}, p, \lambda)$ the solution of problem (5) defined in theorem 2.2. Let $(\mathbf{v}_h, p_h, \lambda_H)$ the solution of (27) with initial data $(\mathbf{v}_{h,0}, p_{h,0})$ the two first components of $\Pi_h(\mathbf{v}_0, p_0, 0)$. Then, we have the error estimates*

$$\left|\begin{array}{l} \|\mathbf{v}_h - \mathbf{v}\|_{C^0([0,T];\underline{L^2}(C))} + \|p_h - p\|_{C^0([0,T];M)} \;\leq \\ \qquad \mathcal{C}(1+T)\left(\|\widehat{\mathbf{v}}_h - \mathbf{v}\|_{C^1([0,T];\underline{L^2}(C))} + \|\widehat{p}_h - p\|_{C^1([0,T];M)}\right) \;+ \\ \qquad \mathcal{C}\,\sqrt{T}\,\|\sqrt{\beta}\|_{L^\infty(C)}\,\|P_{M_h^r}(\widehat{p}_h)\|_{C^0([0,T];M)}. \end{array}\right. \tag{45}$$

Furthermore, if $(\mathbf{v}, p) \in C^2\left([0,T]; \underline{L^2}(C) \times M\right)$ then

$$\left|\begin{array}{l} \|\mathbf{v}_h - \mathbf{v}\|_{C^0([0,T];\underline{X})} \;\leq\; \mathcal{C}\,\|\widehat{\mathbf{v}}_h - \mathbf{v}\|_{C^0([0,T];\underline{X})} \;+ \\ \qquad \mathcal{C}\,(1+T)(1+\|\beta\|_{L^\infty(C)})\left(\|\widehat{\mathbf{v}}_h - \mathbf{v}\|_{C^2([0,T];\underline{L^2}(C))} + \|\widehat{p}_h - p\|_{C^2([0,T];M)}\right) \;+ \\ \qquad \|\beta\|_{L^\infty(C)}(1 \;+\; \sqrt{T}\,\|\sqrt{\beta}\|_{L^\infty})\,\|P_{M_h^r}(\widehat{p}_h)\|_{C^1([0,T];M)}, \end{array}\right. \tag{46}$$

$$\left|\begin{array}{l} \|\lambda_H - \lambda\|_{C^0([0,T];\mathcal{G})} \;\leq\; \mathcal{C}\,\|\widehat{\lambda_H} - \lambda\|_{C^0([0,T];\mathcal{G})} \;+ \\ \qquad \mathcal{C}\,(1+T)\left(\|\widehat{\mathbf{v}}_h - \mathbf{v}\|_{C^2([0,T];\underline{L^2}(C))} + \|\widehat{p}_h - p\|_{C^2([0,T];M)}\right) \;+ \\ \qquad \mathcal{C}\,\sqrt{T}\,\|\sqrt{\beta}\|_{L^\infty}\,\|P_{M_h^r}(\widehat{p}_h)\|_{C^1([0,T];M)}. \end{array}\right. \tag{47}$$

Proof. First, notice that the choice done for the approximate initial data implies $\mathcal{E}_h(0) = 0$. Then inequality (44) easily implies (45). This gives an error estimate for $\mathbf{v}$ in the L^2 norm. In order to obtain an estimate in the $\underline{X}$ norm, we first state a similar result for the time derivative of the solution. Assuming that the solution is one order more regular, then

$$\begin{array}{l} \|\partial_t(\mathbf{v}_h - \mathbf{v})\|_{C^0([0,T];\underline{L^2}(C))} + \|\partial_t(p_h - p)\|_{C^0([0,T];M)} \;\leq \\ \qquad \mathcal{C}(1+T)\left(\|\partial_t(\widehat{\mathbf{v}}_h - \mathbf{v})\|_{C^1([0,T];\underline{L^2}(C))} + \|\partial_t(\widehat{p}_h - p)\|_{C^1([0,T];M)}\right) \;+ \\ \qquad \mathcal{C}\,\sqrt{T}\,\|\sqrt{\beta}\|_{L^\infty(C)}\,\|P_{M_h^r}(\partial_t\widehat{p}_h)\|_{C^0([0,T];M)}. \end{array} \tag{48}$$

Making the difference between the second equation of (27) and the second equation of (5) we obtain

$$(\mathrm{div}(\mathbf{v}_h - \mathbf{v}), q_h) \;\; = \;\; (\partial_t(p_h - p), q_h)_\rho \;+\; (\beta P_{M_h^r}(p_h), q_h), \qquad \forall\, q_h \in M_h.$$

This implies ($\mathrm{div}(\mathbf{v}_h - \widehat{\mathbf{v}}_h) \in M_h$)

$$\|\mathrm{div}(\mathbf{v}_h - \widehat{\mathbf{v}}_h)\|_{L^2(C)} \;\; \leq \;\; \mathcal{C}\left(\|\partial_t(p_h - p)\|_M \;+\; \|\mathrm{div}(\widehat{\mathbf{v}}_h - \mathbf{v})\|_{L^2(C)} \;+\; \|\beta P_{M_h^r}(p_h)\|_M\right),$$

and therefore

$$\begin{aligned}\|\mathrm{div}(\mathbf{v}_h-\mathbf{v})\|_{L^2(C)} &\leq \mathcal{C}\left(\|\partial_t(p_h-p)\|_{C^0([0,T];M)} + \|\widehat{\mathbf{v}}_h-\mathbf{v}\|_{C^0([0,T];\underline{X})}\right) + \\ &\mathcal{C}\|\beta\|_{L^\infty(C)}\left(\|\widehat{p}_h-p\|_M + \|p_h-p\|_M + \right. \\ &\left.\|P_{M_h^r}(\widehat{p}_h)\|_{C^0([0,T];M)}\right).\end{aligned}$$

Then using (45) and (48) we obtain (46). It remains to obtain the estimate for the Lagrange multiplier. Due to the uniform discrete inf-sup condition (31) applied to $\lambda_H-\widehat{\lambda_H}$, there exists $\mathbf{w}_h\in\underline{X}_h$ such that

$$\begin{aligned}\mathcal{C}\|\lambda_H-\widehat{\lambda_H}\|_{\mathcal{G}}\,\|\mathbf{w}_h\|_{\underline{X}} &\leq <\mathbf{w}_h\cdot\mathbf{n},\lambda_H-\widehat{\lambda_H}>_\Gamma \\ &= <\mathbf{w}_h\cdot\mathbf{n},\lambda_H-\lambda>_\Gamma + <\mathbf{w}_h\cdot\mathbf{n},\lambda-\widehat{\lambda_H}>_\Gamma \\ &= a(\partial_t(\mathbf{v}_h-\mathbf{v}),\mathbf{w}_h) + b(\mathbf{w}_h,p_h-p) + <\mathbf{w}_h\cdot\mathbf{n},\lambda-\widehat{\lambda_H}>_\Gamma .\end{aligned}$$

This implies that

$$\|\lambda_H-\lambda\|_{\mathcal{G}} \leq \mathcal{C}\left(\|\lambda-\widehat{\lambda_H}\|_{\mathcal{G}(\Gamma)} + \|\partial_t(\mathbf{v}_h-\mathbf{v})\|_{\underline{L^2}(C)} + \|p_h-p\|_M\right),$$

and therefore, using (45) and (48) we show estimate (47). □

Finally, the following theorem gives the order of convergence of the method.

Theorem 5.6 *We make the same assumptions as in theorem 5.5. Then we have*

- *if* $(\mathbf{v},p,\lambda)\in C^1\left([0,T];H^{\frac12-\varepsilon}(\mathrm{div},C)\times H^{\frac12-\varepsilon}(C)\times H^{1-\varepsilon}(\Gamma)\right)$

$$\left|\begin{array}{l}\|\mathbf{v}_h-\mathbf{v}\|_{C^0([0,T];\underline{L^2}(C))}+\|p_h-p\|_{C^0([0,T];M)} \leq \mathcal{C}\left(h^{\frac12-\varepsilon}+H^{\frac12-\varepsilon}\right)\\ \qquad\left[(1+T)\left(\|\mathbf{v}\|_{C^1([0,T];H^{\frac12-\varepsilon}_{div}(C))}+\|p\|_{C^1([0,T];H^{\frac12-\varepsilon}(C))}+\|\lambda\|_{C^1([0,T];H^{1-\varepsilon}(\Gamma))}\right)+\right.\\ \left.\sqrt{T}\|\sqrt{\beta}\|_{L^\infty(C)}\left(\|\mathbf{v}\|_{C^0([0,T];H^{\frac12-\varepsilon}_{div}(C))}+\|p\|_{C^0([0,T];H^{\frac12-\varepsilon}(C))}+\|\lambda\|_{C^0([0,T];H^{1-\varepsilon}(\Gamma))}\right)\right],\end{array}\right. \tag{49}$$

- *if* $(\mathbf{v},p,\lambda)\in C^2\left([0,T];H^{\frac12-\varepsilon}(\mathrm{div},C)\times H^{\frac12-\varepsilon}(C)\times H^{1-\varepsilon}(\Gamma)\right)$

$$\left|\begin{array}{l}\|\mathbf{v}_h-\mathbf{v}\|_{C^0([0,T];\underline{X})} \leq \mathcal{C}\left(h^{\frac12-\varepsilon}+H^{\frac12-\varepsilon}\right)(1+T)\left(1+\|\beta^{\frac32}\|_{L^\infty(C)}\right)\\ \qquad\left(\|\mathbf{v}\|_{C^2([0,T];H^{\frac12-\varepsilon}_{div}(C))}+\|p\|_{C^2([0,T];H^{\frac12-\varepsilon}(C))}+\|\lambda\|_{C^2([0,T];H^{1-\varepsilon}(\Gamma))}\right),\end{array}\right. \tag{50}$$

$$\left|\begin{array}{l}\|\lambda_H-\lambda\|_{C^0([0,T];\mathcal{G})} \leq \mathcal{C}\left(h^{\frac12-\varepsilon}+H^{\frac12-\varepsilon}\right)\\ \qquad\left[(1+T)\left(\|\mathbf{v}\|_{C^2([0,T];H^{\frac12-\varepsilon}_{div}(C))}+\|p\|_{C^2([0,T];H^{\frac12-\varepsilon}(C))}+\|\lambda\|_{C^2([0,T];H^{1-\varepsilon}(\Gamma))}\right)+\right.\\ \left.\sqrt{T}\|\sqrt{\beta}\|_{L^\infty(C)}\left(\|\mathbf{v}\|_{C^1([0,T];H^{\frac12-\varepsilon}_{div}(C))}+\|p\|_{C^1([0,T];H^{\frac12-\varepsilon}(C))}+\|\lambda\|_{C^1([0,T];H^{1-\varepsilon}(\Gamma))}\right)\right].\end{array}\right. \tag{51}$$

Proof. This is a consequence of estimates on the evolution problem obtained in 5.5 combined with the estimates obtained on the elliptic projection error in corollary 5.2. □

6 Numerical error estimates

In this section we are interested in estimating numerically the order of convergence of the method. To do so, we consider solving the wave equation on a disk $\Omega \subset I\!R^2$ with homogeneous Neumann boundary conditions on its boundary $\Gamma = \partial\Omega$. The geometry of the problem is presented in Figure 6.

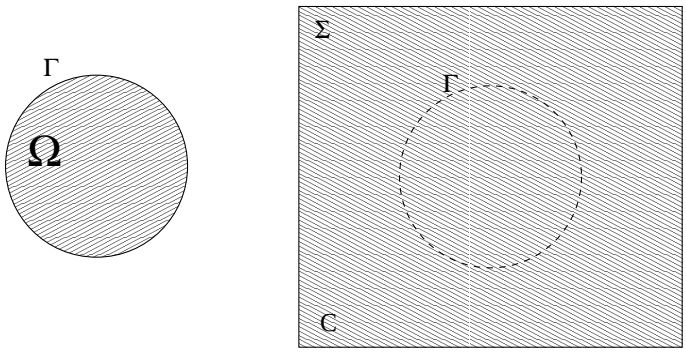

Figure 6: The geometry of the problem. On the left the initial domain of propagation Ω and on the right the extended domain, C, introduced by the fictitious domain formulation of the problem.

To compute the solution we extend the unknowns in the domain of simple geometry C (see Figure 6) and use the fictitious domain formulation (5) with a zero force term $f = 0$ and the initial conditions given in section 3.2. The center of the initial condition, $(x_c, z_c) = (5, 5)$mm, coincides with the center of the disk Ω whose radius is $R = 4mm$. The physical properties of the material and size of the computational domain are the same as in section 3.2. In practice to truncate the extended domain C, we surround the computational domain by a perfectly matched absorbing layer model (PML, [7, 11]).

We remark that the solution of this problem is rotationally invariant because of the symmetry in the geometry and the initial conditions. We use this symmetry in order to compute a reference solution by solving an one dimensional problem. More precisely, when expressed in cylindrical coordinates, it is easy to see that the solution of the two dimensional problem, (Ω being $[0, R]\times[0, 2\pi]$, and where $\varrho = 1000$Kgr/m^3 and $a = 10^9$Pa),

$$\left|\begin{array}{ll} a\dfrac{\partial v_r}{\partial t} - \dfrac{\partial p}{\partial r} = 0, & \text{in } [0, R] \times [0, 2\pi], \\ a\dfrac{\partial v_\theta}{\partial t} - \dfrac{\partial p}{\partial \theta} = 0, & \text{in } [0, R] \times [0, 2\pi], \\ \varrho\dfrac{\partial p}{\partial t} - \dfrac{\partial v_r}{\partial r} - \dfrac{1}{r}v_r = 0, & \text{in } [0, R] \times [0, 2\pi], \\ v_r = 0, & \text{on } [r = R] \times [0, 2\pi], \end{array}\right.$$

with initial conditions,

$$p_0(r, \theta) = 0.1F(r/r_0),\ v_r = v_\theta = 0,$$

depends only on r, i.e., $v_r(r, \theta) = v_r(r), v_\theta = 0,\ p(r, \theta) = p(r)$. Thus, it can be deduced by solving the following one-dimensional problem,

$$\left|\begin{array}{ll} a\dfrac{\partial v_r}{\partial t} - \dfrac{\partial p}{\partial r} = 0, & \text{in } [0, R], \\ \varrho\dfrac{\partial p}{\partial t} - \dfrac{\partial v_r}{\partial r} - \dfrac{1}{r}v_r = 0, & \text{in } [0, R], \\ v_r = 0, & \text{for } r = 0 \text{ and } r = R, \end{array}\right. \tag{52}$$

with initial conditions,

$$p(r, t = 0) = 0.1F(r/r_0),\ v_r(t = 0, r) = 0.$$

To solve numerically the one dimensional problem (52), we use piecewise constant functions for the discretization of p_r and continuous piecewise linear functions for v_r. For the time discretization a second order leap frog scheme is employed.

In figure 7 we display the results of the numerical convergence analysis. The reference solution in 1D, is obtained on a fine grid with a space discretization step $h_{1d} = 1/160$mm. The two dimensional problem is solved with four different discretizations using $h_x = h_z = h = 1/10, 1/20, 1/40$ and $1/80$mm. For each discretization we compute the difference between the obtained solution and the reference one. In figure 7 we display the logarithm of the error as a function of the logarithm of the discretization step. The rate of convergence is deduced from the slope s of the line. We can remark that the results obtained numerically are slightly better than our theoretical predictions. Note however, that the estimate obtained on the $L^\infty([0,T], H(\mathrm{div}))$ norm of $\mathbf{v}$ is $h^{0.48}$ which indicates that the theoretical estimations are optimal.

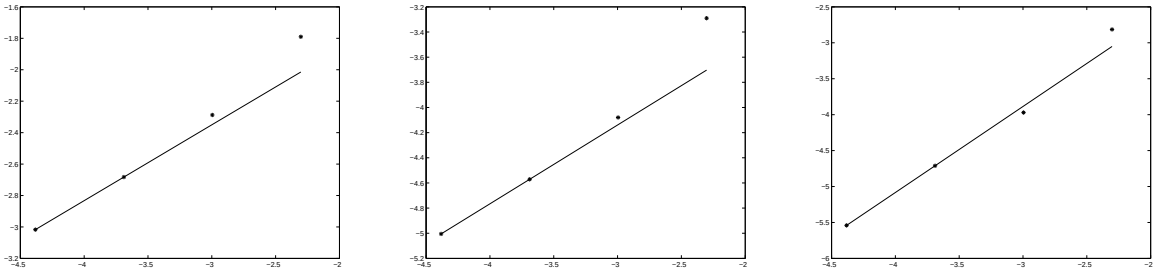

(a) $\sup_{t\leq T} \|\mathbf{v}-\mathbf{v}_h\|_{\underline{X}}$, $s = 0.48$. (b) $\sup_{t\leq T} \|p-p_h\|_M$, $s = 0.63$. (c) $\sup_{t\leq T} \|\lambda-\lambda_h\|_{\mathcal{G}}$, $s = 1.2$.

Figure 7: Numerical error on $\mathbf{v}$, p and λ versus the discretization step.

In figure 8 we display the same results but with the norm of the error now computed in $\widetilde{C} = C/B_b(\Gamma)$, i.e., the domain C restricted from $B_b(\Gamma)$, defined by

$$B_b(\Gamma) = \left\{ \mathbf{x} \in C \text{ s.t. } \min_{\mathbf{y}\in\Gamma} |\mathbf{x}-\mathbf{y}| \leq b \right\}. \tag{53}$$

We observe that the convergence rate of the method is higher, actually one approximately recovers the order of convergence of the method without obstacle, here $O(h)$. Furthermore, we remarked numerically that $b = h$ is the critical value, i.e., the convergence rate does not change for bigger values of b and it decreases for $b < h$. This agrees with our intuition in the sense that the elements that we need to remove are the ones in which the solution has less regularity (see remark 1), i.e., the elements that have non-zero intersection with the boundary Γ. Finally, notice that the rate of convergence on λ (approximately 1) is higher than expected (1/2). We conjecture that this is due to the closed boundary and that this rate would be lower for an open boundary (see remark 1).

7 Extension to the elastodynamic case

We consider in this section the problem of elastic wave scattering by a crack. The generalization of the fictitious domain method to this case was presented in [5]. For the space discretization of the volume unknowns, which are in this case the stress tensor and the velocity field, an original finite element method was proposed and analyzed in [6]. The lower order elements of this family coupled with piecewise linear continuous elements for the surface unknown were used in [5]. This choice corresponds to the vectorial analogue of the $Q_1^{div} \times Q_0$ element coupled with P_1 continuous elements on the crack that was discussed in section 3. Also here, the same questions and difficulties arise. Namely, from the theoretical point of view, the convergence of the method

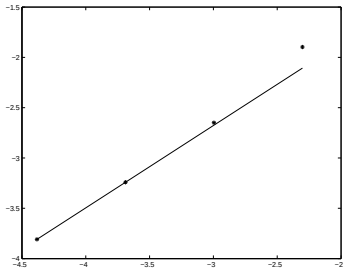

(a) $\sup_{t\leq T} \|\mathbf{v}-\mathbf{v}_h\|_{\underline{H_{div}}(\widetilde{C})}$. $s=0.82$.

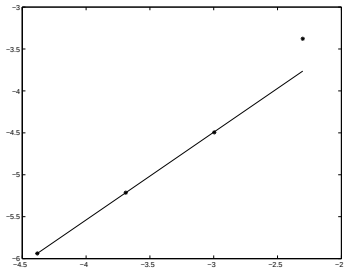

(b) $\sup_{t\leq T} \|p-p_h\|_{L^2(\widetilde{C})}$. $s=1$.

Figure 8: Numerical error on $\mathbf{v}$, p and λ versus the discretization step. Here we compute the norm of the error in the domain $\widetilde{C}$ which is C restricted from $B_b(\Gamma)$, i.e., Γ and its vicinity (53).

was not proved and numerical examples indicate that for some crack geometries the method does not converge. The solution we propose is to use instead the modified $Q_1^{div} \times P_1^{disc}$ element. As for the case without crack, the theoretical convergence of the method is not a straightforward generalization of the scalar case. The main difficulty in generalizing the results presented in section 5 is the proof of the inf-sup condition (31). Although this condition was not shown theoretically we will show numerical results that indicate the convergence of the method. Let us remark that the inf-sup condition is sufficient and not necessary for the convergence of the method. See [4] or [6] for examples where the convergence holds under weaker conditions.

We briefly present in the following the continuous elastodynamic problem, the finite elements used for the space discretization and the numerical results obtained in this case.

7.1 The continuous problem

Consider the geometry given in Fig. 1 and assume now that the material filling Ω is an elastic solid. In this case, and under the assumption of small deformations, wave propagation is governed by the linear elastic wave equations,

$$
\left\{
\begin{array}{l}
\text{Find } (\boldsymbol{\sigma},\mathbf{v}) : (x,t)\in\Omega\times[0,T]\mapsto(\boldsymbol{\sigma}(x,t),\mathbf{v}(x,t))\in\mathbb{R}^4\times\mathbb{R}^2 \text{ satisfying,}\\
\rho\dfrac{\partial \mathbf{v}}{\partial t} - \text{div}\,\boldsymbol{\sigma} = \mathbf{f}, \qquad \text{in } \Omega, \qquad (a)\\
\mathbf{A}\dfrac{\partial \boldsymbol{\sigma}}{\partial t} - \boldsymbol{\varepsilon}(\mathbf{v}) = 0, \qquad \text{in } \Omega, \qquad (b)\\
\boldsymbol{\sigma}\mathbf{n} = 0, \qquad \text{on } \Gamma, \qquad (c)\\
\mathbf{v} = 0, \qquad \text{on } \Sigma, \qquad (d)
\end{array}
\right. \tag{54}
$$

together with the initial conditions,

$$
\left\{
\begin{array}{ll}
\mathbf{v}(t=0) = \mathbf{v}_0,\\
\boldsymbol{\sigma}(t=0) = \boldsymbol{\sigma}_0.
\end{array}
\right. \tag{55}
$$

In (54), $\mathbf{v}$ is the velocity field and $\boldsymbol{\sigma}$ the stress tensor. This formulation is preferred to the classical displacement formulation because the boundary condition on the crack is natural (of Neumann type) for the displacement while it becomes essential on $\boldsymbol{\sigma}$ and the fictitious domain approach can then be followed. Note that the couple $(\boldsymbol{\sigma},\mathbf{v})$ plays the same role here as the couple $(\mathbf{v},p)$ in the scalar case. The matrix $\mathbf{A}$ becomes now a fourth-order symmetric definite positive tensor.

The fictitious domain formulation, analogous to (5) for the scalar problem, is

$$
(56)\qquad \left\{
\begin{array}{l}
\text{Find } (\boldsymbol{\sigma}(t),\mathbf{v}(t),\boldsymbol{\lambda}(t)) \in \underline{\underline{X}}^{sym} \times \underline{M} \times \underline{\mathcal{G}} \text{ satisfying,} \\
\dfrac{\mathrm{d}}{\mathrm{d}t}a(\boldsymbol{\sigma},\boldsymbol{\tau}) + b(\boldsymbol{\tau},\mathbf{v}) - <\boldsymbol{\tau}\mathbf{n},\boldsymbol{\lambda}>_\Gamma = 0, \quad \forall \boldsymbol{\tau} \in \underline{\underline{X}}^{sym}, \\
\dfrac{\mathrm{d}}{\mathrm{d}t}(\mathbf{v},\mathbf{w})_\rho - b(\boldsymbol{\sigma},\mathbf{w}) = (\mathbf{f},\mathbf{w}), \quad \forall \mathbf{w} \in \underline{M}, \\
<\boldsymbol{\sigma}\mathbf{n},\boldsymbol{\mu}>_\Gamma = 0, \quad \forall \boldsymbol{\mu} \in \underline{\mathcal{G}}, \\
(\boldsymbol{\sigma},\mathbf{v})_{/t=0} = (\boldsymbol{\sigma}_0,\mathbf{v}_0),
\end{array}
\right.
$$

where the bilinear forms are defined by (6) with the obvious changes. The functional spaces are defined by

$$\underline{\underline{X}}(=\underline{\underline{X}}(C)) = \underline{X} \times \underline{X}, \quad \underline{M} = M \times M, \quad \underline{\mathcal{G}} = \mathcal{G} \times \mathcal{G},$$

the stress tensor belonging to the subspace of symmetric tensors in $\underline{\underline{X}}$,

$$\underline{\underline{X}}^{sym} = \left\{\sigma \in \underline{\underline{X}} \,/\, \mathrm{as}(\sigma) = 0\right\},$$

with $\mathrm{as}(\sigma)$ defined in 2D by,

$$\mathrm{as}(\sigma) = \sigma_{12} - \sigma_{21}.$$

The generalization of the existence and uniqueness results presented in section 2 to this problem is straightforward.

7.2 The approximate problem

The semi-discrete formulation For the approximation in space of this problem, we introduce finite dimensional spaces $\underline{\underline{X_h}}^{sym} \subset \underline{\underline{X}}^{sym}$, $\underline{M_h} \subset \underline{M}$ and $\underline{\mathcal{G}_H} \subset \underline{\mathcal{G}}$ satisfying the usual approximation properties,

$$
(57)\qquad \left|
\begin{array}{ll}
\inf\limits_{h\geq 0}\inf\limits_{\boldsymbol{\tau}_h \in \underline{\underline{X_h}}^{sym}} \|\boldsymbol{\tau}-\boldsymbol{\tau}_h\|_{\underline{\underline{X}}} = 0, & \forall \boldsymbol{\tau} \in \underline{\underline{X}}^{sym}, \\
\inf\limits_{h\geq 0}\inf\limits_{\mathbf{v}_h \in \underline{M_h}} \|\mathbf{v}-\mathbf{v}_h\|_{\underline{M}} = 0, & \forall \mathbf{v} \in \underline{M}, \\
\inf\limits_{H\geq 0}\inf\limits_{\boldsymbol{\mu}_H \in \underline{\mathcal{G}_H}} \|\boldsymbol{\mu}-\boldsymbol{\mu}_H\|_{\underline{\mathcal{G}}} = 0, & \forall \boldsymbol{\mu} \in \underline{\mathcal{G}}.
\end{array}
\right.
$$

The semi-discrete problem is then,

$$
(58)\qquad \left\{
\begin{array}{l}
\text{Find } (\boldsymbol{\sigma}_h(t),\mathbf{v}_h(t),\boldsymbol{\lambda}_H(t)) \in \underline{\underline{X_h}}^{sym} \times \underline{M_h} \times \underline{\mathcal{G}_H} \text{ such that,} \\
\dfrac{\mathrm{d}}{\mathrm{d}t}a(\boldsymbol{\sigma}_h,\boldsymbol{\tau}_h) + b(\boldsymbol{\tau}_h,\mathbf{v}_h) - <\boldsymbol{\tau}_h\cdot\mathbf{n},\boldsymbol{\lambda}_H>_\Gamma = 0, \quad \forall \boldsymbol{\tau}_h \in \underline{\underline{X_h}}^{sym}, \\
\dfrac{\mathrm{d}}{\mathrm{d}t}(\mathbf{v}_h,\mathbf{w}_h)_\rho - b(\boldsymbol{\sigma}_h,\mathbf{w}_h) = (f,\mathbf{w}_h), \quad \forall \mathbf{w}_h \in \underline{M_h}, \\
<\boldsymbol{\sigma}_h\cdot\mathbf{n},\boldsymbol{\mu}_H>_\Gamma = 0, \quad \forall \boldsymbol{\mu}_H \in \underline{\mathcal{G}_H}, \\
\boldsymbol{\sigma}_h(t=0) = \boldsymbol{\sigma}_{h,0}, \\
\mathbf{v}_h(t=0) = \mathbf{v}_{h,0},
\end{array}
\right.
$$

and where $(\boldsymbol{\sigma}_{h,0}, p_{h,0}) \in \underline{\underline{X_h}}^{sym} \times \underline{M_h}$ is an approximation of the exact initial condition.

The two families of mixed finite elements. Following the same ideas as for the scalar problem, an original finite element for the elastodynamic system which is compatible with mass lumping was introduced in [6]. The difference with the $Q_{k+1}^{div} - Q_k$ elements is due to the symmetry of the stress tensor. Namely the lowest order element in this case is,

$$\left\{ \begin{array}{l} \underline{\underline{X_h}} = \left\{ \boldsymbol{\tau}_h \in \underline{\underline{X}} / \ \forall K \in \mathcal{T}_h, \ \boldsymbol{\tau}_h|_K \in (Q_1 \times Q_1)^2 \right\}, \\ \underline{\underline{X_h}}^{sym} = \left\{ \boldsymbol{\tau}_h \in \underline{\underline{X_h}} \ / \ \mathrm{as}(\boldsymbol{\tau}_h) = 0 \right\}, \qquad \underline{M_h} = \underline{M_h}^0 = (M_h^0)^2, \end{array} \right. \tag{59}$$

M_h^0 being defined as for the scalar case. Another characterization $\underline{\underline{X_h}}^{sym}$ is

$$\begin{aligned} \underline{\underline{X_h}}^{sym} = \ & \left\{ \sigma_{12} \in H^1(\Omega) / \sigma_{12}|_K \in Q_1, \ \forall K \in \mathcal{T}_h \ \text{ and} \right. \\ & \left. (\sigma_{11}, \sigma_{22}) \in H(\mathrm{div}, \Omega) / (\sigma_{11}, \sigma_{22})|_K \in (Q_1)^2, \ \forall K \in \mathcal{T}_h \right\}. \end{aligned} \tag{60}$$

The degrees of freedom of the lowest order element for the elastic problem are illustrated in Figure 9. We

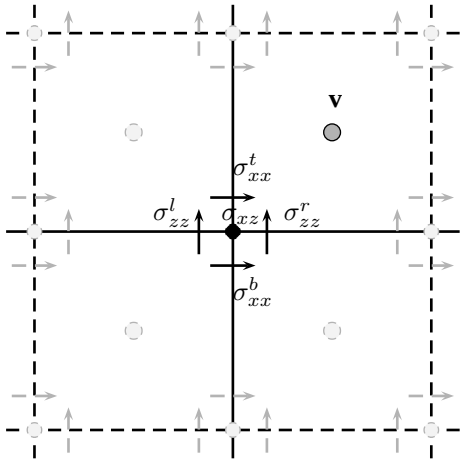

Figure 9: Degrees of freedom for the mixed finite element defined by (59)

obviously do not have $\underline{\underline{X_h}}^{sym} = \underline{X_h} \times \underline{X_h}$. This implies in particular that the approximation space $\underline{\underline{X_h}}^{sym}$ does not a priori contain the lowest order Raviart Thomas element. Moreover the remarks made in the scalar case on the coercivity and the (non-) inclusion property (16) remain true. Therefore, once again the assumptions of the classical mixed finite element theory (cf. [8, 14]) are not satisfied. However, convergence results and error estimates for the problem without Lagrange multiplier were obtained in [6].

We recall here the approximation properties for the space $\underline{\underline{X_h}}^{sym}$. Let $\tau \in \underline{\underline{X}}^{sym}$ with $(\tau_{11}, \tau_{22}) \in H^{1,0} \times H^{0,1}$ (see [6] for the definition of these spaces), and $\tau_{12} = \tau_{21} \in H^1$ then

$$\lim_{h \to 0} \inf_{\boldsymbol{\tau}_h \underline{\underline{X_h}}^{sym}} \|\boldsymbol{\tau} - \boldsymbol{\tau}_h\|_{\underline{\underline{X}}} = 0.$$

Moreover, if $(\tau_{11}, \tau_{22}) \in H^{2,1} \times H^{1,2}$ and $\tau_{12} \in H^2$ then

$$\inf_{\boldsymbol{\tau}_h \in \underline{\underline{X_h}}^{sym}} \|\boldsymbol{\tau} - \boldsymbol{\tau}_h\|_{\underline{\underline{X}}} \leq Ch(|\tau_{11}|_{H^{2,1}} + |\tau_{22}|_{H^{1,2}} + |\tau_{12}|_{H^2}). \tag{61}$$

The approximation of the Lagrange multiplier is done in the space $\underline{\mathcal{G}_H} = (\mathcal{G}_h)^2$, $\mathcal{G}_h$ being defined by (14). The spaces $(\underline{M_h}^0, \underline{\mathcal{G}_H})$ satisfy the usual approximation properties (10).

The choice of the above approximation spaces seemed once again reasonable. However, as for the scalar case no theoretical convergence results were obtained for the fictitious domain formulation. Moreover, numerical examples indicate that for some crack geometries the method does not converge.

As a response to this drawback, the same approach as for the scalar case was followed. The modified element consists in this case to discretize the velocity in $\underline{M_h}^1 = (M_h^1)^2$. From the numerical point of view this choice introduces spurious modes in the velocity whose amplitude is more important than in the acoustic case. The selective damping of the spurious modes is achieved using the same tools as in section 4.4. Namely, the second equation of (58) is replaced by

$$\frac{\mathrm{d}}{\mathrm{d}t}(\mathbf{v}_h, \mathbf{w}_h)_\rho + (P_{\underline{M_h}^r}(\mathbf{v}_h), \mathbf{w}_h)_\beta - b(\boldsymbol{\sigma}_h, \mathbf{w}_h) = (f, \mathbf{w}_h), \quad \forall \mathbf{w}_h \in \underline{M_h},$$

where $\underline{M_h}^r = (M_h^r)^2$ and β is the damping parameter.

Convergence issues. From the numerical point of view we observe that the method converges under a compatibility condition of the form (15) between the two discretization meshes. From the theoretical point of view the convergence proof in this case is not a straightforward generalization of the results in section 5. The main difficulty comes from the non standard regularity required to obtain the approximation properties for $\underline{\underline{X_h}}^{sym}$ (see (61)). Indeed, the maximal regularity (in space) of the stress tensor in the case of a domain with a crack is $\boldsymbol{\sigma} \in (H^{\frac{1}{2}-\varepsilon}(\mathrm{div}, C))^2$, and $\boldsymbol{\sigma}$ is symmetric. This regularity is not sufficient to obtain (61) and thus we cannot conclude.

8 Numerical illustrations

We present in what follows some numerical results that illustrate the difficulties related with the convergence of the method that we discussed in the previous section.

The computational domain is again the square $[0, 10] \times [0, 10]\ mm^2$ composed by an homogeneous isotropic material with density and Lame coefficients given by

$$\rho = 1000\ \text{Kgr/m}^3, \quad \lambda = 3.45 \times 10^9\ \text{Pa}, \quad \mu = 2.04 \times 10^9\ \text{Pa}. \tag{62}$$

We introduce an initial condition on the velocity field centered on $(x_c, z_c) = (5, 5)$mm,

$$\mathbf{v}((x, z), t = 0) = 0.1\ F\left(\frac{r}{r_0}\right)\frac{\mathbf{r}}{r},$$

where $F(\cdot)$, $\mathbf{r}$ and r have been defined in section 3.2 and $r_0 = 1.5$mm. We consider the diagonal crack parameterized by (18) on which we impose a free surface boundary condition. We use a mesh composed by squares with a discretization step $h = 0.025$mm. For the time discretization we use again a leap frog scheme with a time step Δt such that the ratio $\Delta t/h$ is equal to the maximal value that guarantees the stability. The crack is also discretized using a regular mesh with $H = 1.2h$. Perfectly matched layers are used to bound the computational domain.

Results with the $Q_1^{div} \times Q_0$ element. When we use the original finite element, the incident wave (which is here a pressure wave) is not completely reflected by the obstacle but also transmitted as it can be clearly seen in figure 10-(a). Similar results are also obtained when using other ratios between H and h and when refining the meshes. This indicates a lack of convergence as in the scalar case.

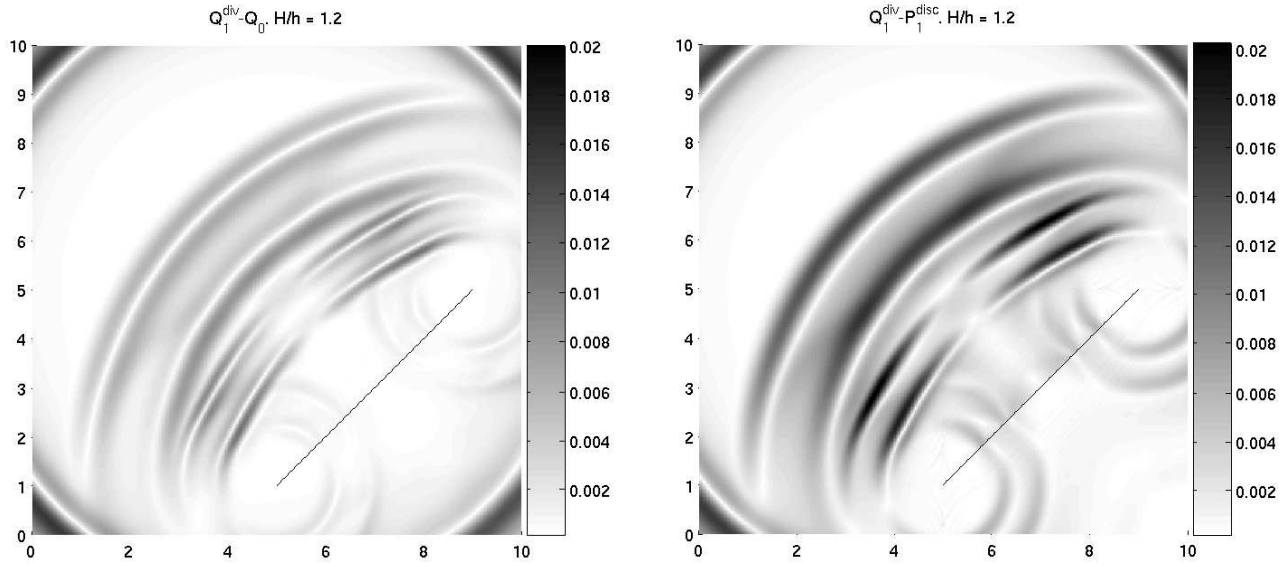

(a) $Q_1^{div} \times Q_0$ (b) $Q_1^{div} \times P_1^{disc}$

Figure 10: Modulus of the velocity field at $t = 2.5965$ μs.

Results with the $Q_1^{div} \times P_1^{disc}$ element. The solution obtained with the new finite element seems to converge towards the solution of the continuous problem. The incident wave is completely reflected by the obstacle and the scattered waves generated by the extremities of the crack are well approximated (see figure 10-(b)). As in the scalar case, the enrichment of the $\underline{M_h}$ approximation space introduces spurious modes in the solution. Although the amplitude of these non-physical waves goes to zero with the size of the discretization step, it is still significant for a usual choice of the discretization parameters, typically corresponding to 20 points per wavelength. These spurious modes are for example visible in the results presented in figure 11-(a) where we have amplified by a factor eight the results of figure 10-(b). In order to study in more detail these phenomena we represent in figure 12 the evolution in time of the modulus of the velocity field at three points: $\mathbf{x_1} = (x_1, z_1) = (6.5, 3.5)$mm, $\mathbf{x_2} = (x_2, z_2) = (7.5, 2.5)$mm and $\mathbf{x_3} = (x_3, z_3) = (5, 0.5)$mm. The first two points are centered with respect to the crack, one behind and the other in front of it. The third point is located near the lower tip of the crack, where the spurious waves seem stronger. To determine the speed of convergence of the method, we use three different meshes with a space discretization step of $h = 0.025, 0.0125$ and 0.00625mm.

The results obtained at the first point (in front of the crack) are already good with the coarse mesh (see figure 12-top left). The amplitude of the spurious waves is very small with respect to the amplitude of the incident ($t \in [0.25, 1]$ μs), reflected ($t \in [0.75, 2]$ μs) and (first) scattered wave ($t \in [2.75, 4.25]$ μs).

The second point is in the "shadow region" where the amplitude of the physical waves is about 15% smaller than the amplitude of the incident wave (see figure 12-middle left). Consequently the error is more visible. In the time interval $t \in [0, 2]$ μs we can see the part of the incident wave that has been transmitted across the obstacle. The amplitude of those waves goes to zero when we refine the mesh. From $t = 2$ to $t = 4.5$ μs we can see the first group of scattered waves. At the beginning and at the end of this time interval we can see some oscillations that come from the spurious modes introduced by the enrichment of the velocity field discretization space. The error on those amplitudes is about 2% of the amplitude of the incident wave.

At the third point, the spurious phenomena are much stronger (see figure 12-bottom left). Here, the amplitude of the incident and scattered waves is about 40% of the amplitude of the actual incident wave. As we can

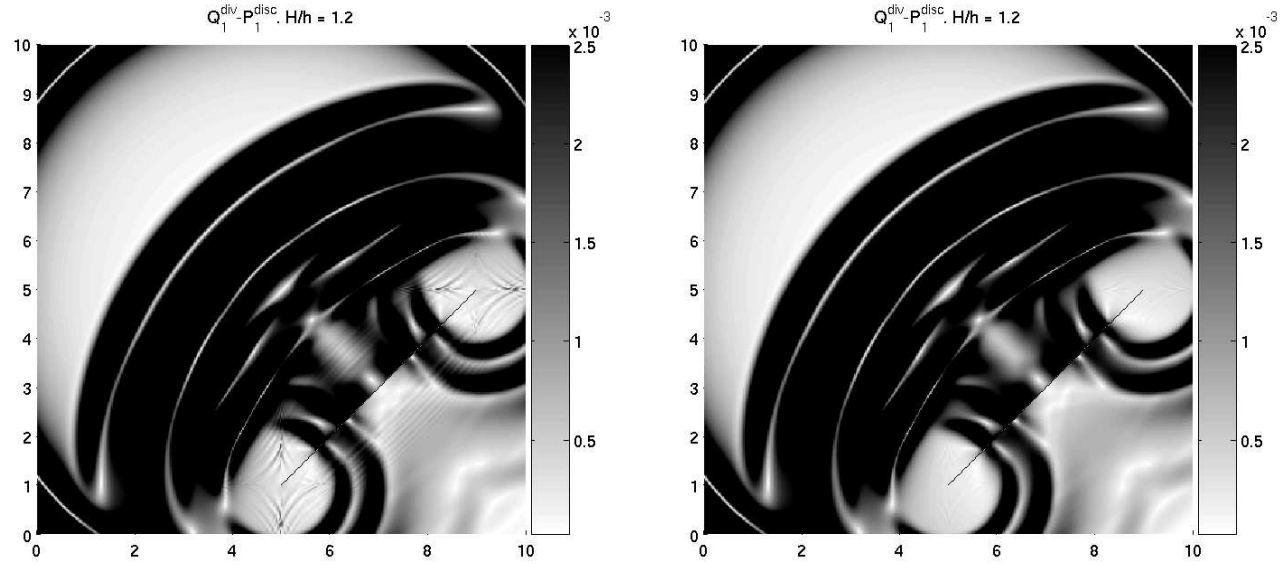

(a) $Q_1^{div} \times P_1^{disc},\ \beta = 0$

(b) $Q_1^{div} \times P_1^{disc},\ \beta = 5\varrho 10^6$

Figure 11: Modulus of the velocity field $\times 8$ at $t = 2.5965\ \mu$s.

observe, comparing the solutions obtained with the different meshes, the method converges very slowly (see the time interval $t \in [2, 5.5]\ \mu$s). That is the effect of the spurious modes created by the singularity on the tips of the crack (see also figure 11-(a)).

These spurious phenomena can be reduced using a positive value of β, the damping coefficient. Let us analyze the results obtained with $\beta = 5\varrho 10^6$. As we can see in figure 11-(b) the results seem to be better than those obtained with $\beta = 0$ (see figure 11-(a)). The signal obtained at the first point $\mathbf{x_1}$ is very similar for both choices (see figure 12-top right). The results for the second point are also comparable. We remark that some oscillations on the time intervals $t \in [2, 3]$ and $t \in [4.5, 6]$ are removed with the damping. It is in the signal recorded on the third point where the effect of the damping of the spurious modes is more efficient (see figure 12-bottom right). The oscillations observed with $\beta = 0$ are completely removed and the method gives a good solution even with the coarsest mesh.

Influence of the damping parameter on the solution. To illustrate the effect of the damping parameter β on the solution we present in figure 13 results obtained on the coarsest grid for different values of β. We have made the following observations: when we do not use any damping, the solution is polluted by spurious modes. On the other hand, the amplitude of the transmitted (non-physical) waves through the crack increases as the value of the damping β increases. This is expected because the limit case $\beta \to +\infty$ corresponds to seeking the velocity in Q_0 and we know that in this case, the method does not converge. There is thus an optimal value for the damping parameter β to be determined so as the spurious modes are damped while the transmitted non-physical wave remains small. In the next section we determine numerically the rate of convergence of the method for a particular geometry and we discuss a procedure to choose the value of β.

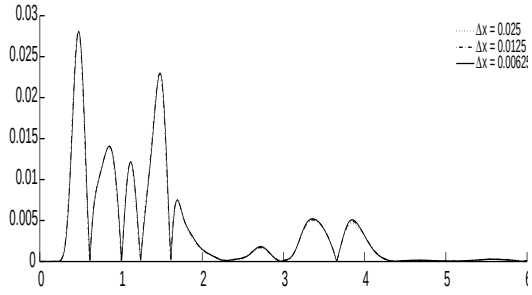

(a) $|v|((6.5, 3.5)mm, t)$, $\beta = 0$

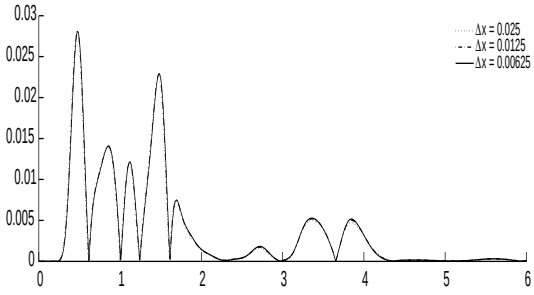

(b) $|v|((6.5, 3.5)mm, t)$, $\beta = 5\varrho 10^6$

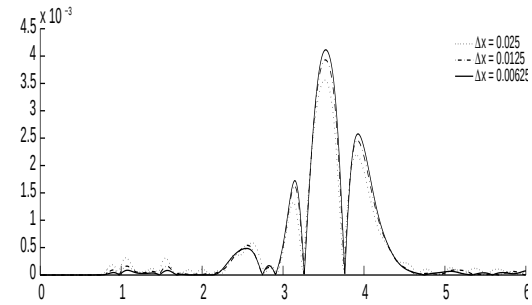

(c) $|v|((7.5, 2.5)mm, t)$, $\beta = 0$

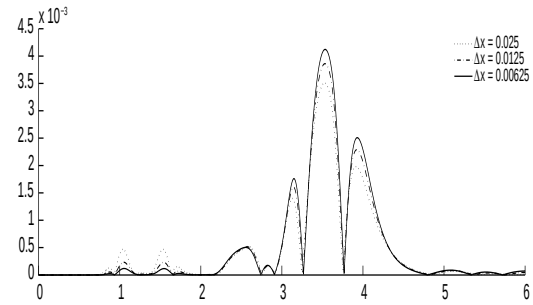

(d) $|v|((7.5, 2.5)mm, t)$, $\beta = 5\varrho 10^6$

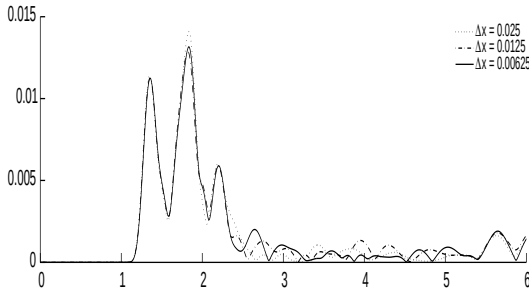

(e) $|v|((5.0, 0.5), t)$, $\beta = 0$

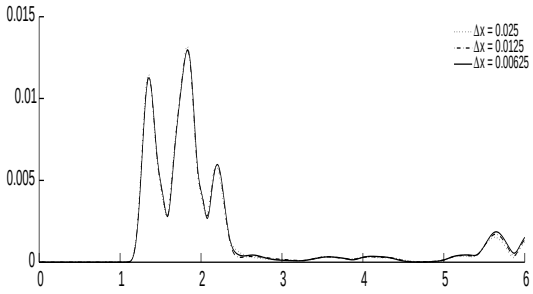

(f) $|v|((5.0, 0.5), t)$, $\beta = 5\varrho 10^6$

Figure 12: The modulus of the velocity $|\mathbf{v}|(\mathbf{x_i}, t),\ t \in [0, 6],\ i \in \{1, 2, 3\}$ computed using the $Q_1^{div} \times P_1^{disc}$ element with $\beta = 0$ on the left column and $\beta = 5\varrho 10^6$ on the right one.

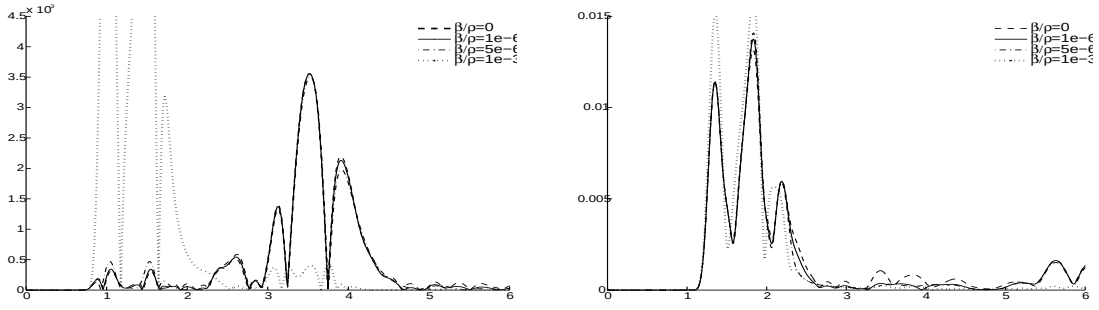

(a) $|v|((7.5, 2.5)\text{mm}, t)$ (b) $|v|((5.0, 0.5)\text{mm}, t)$

Figure 13: The modulus of the velocity $|\mathbf{v}|(\mathbf{x_i}, t),\ t \in [0, 6]\mu\text{s},\ i \in \{2, 3\}$ computed using the $Q_1^{div} \times P_1^{disc}$ element with $h = 0.025$mm and different values of the damping parameter β.

9 Numerical error estimates

In the same way as for the scalar case, we determine numerically the order of convergence of the fictitious domain method applied to elastodynamics. To do so we consider the geometry in section 6 with $R = 4$ mm, no external forces and an initial condition on the velocity field given by

$$\mathbf{v}((x, z), t = 0) \quad = \quad 0.1\ F\left(\frac{r}{r_0}\right)\frac{\mathbf{r} + \mathbf{r}^{\perp}}{r},$$

where $F(\cdot)$, $\mathbf{r}$ and r have been defined in section 3.2 and $r_0 = 1.5mm$. The domain of propagation is an isotropic medium with the density and Lame coefficients given by (62). The extended domain C introduced by the fictitious domain formulation is truncated using perfectly matched layers (PML, [7, 11]). We consider the final time equal to $T = 5\mu s$ when both, the pressure and shear waves have reached the boundary.

The fact of having a problem that is rotationally invariant allows us to compute a reference solution solving a one dimensional problem. More precisely, rewriting equations (54) in polar coordinates

$$\left|\begin{array}{rcll}
\rho\dfrac{\partial v_r}{\partial t} & = & \dfrac{\partial \sigma_{rr}}{\partial r} + \dfrac{1}{r}\dfrac{\partial \sigma_{r\theta}}{\partial \theta} + \dfrac{1}{r}(\sigma_{rr} - \sigma_{\theta\theta}), & \text{in } [0, R] \times [0, 2\pi], \\
\rho\dfrac{\partial v_\theta}{\partial t} & = & \dfrac{\partial \sigma_{r\theta}}{\partial r} + \dfrac{1}{r}\dfrac{\partial \sigma_{\theta\theta}}{\partial \theta} + \dfrac{2}{r}\sigma_{r\theta}, & \text{in } [0, R] \times [0, 2\pi], \\
\dfrac{\partial \sigma_{rr}}{\partial t} & = & (2\mu + \lambda)\dfrac{\partial v_r}{\partial r} + \lambda\dfrac{v_r}{r} + \lambda\dfrac{1}{r}\dfrac{\partial v_\theta}{\partial \theta}, & \text{in } [0, R] \times [0, 2\pi], \\
\dfrac{\partial \sigma_{\theta\theta}}{\partial t} & = & (2\mu + \lambda)\left(\dfrac{1}{r}\dfrac{\partial v_\theta}{\partial \theta} + \dfrac{v_r}{r}\right) + \lambda\dfrac{\partial v_r}{\partial r}, & \text{in } [0, R] \times [0, 2\pi], \\
\dfrac{\partial \sigma_{r\theta}}{\partial t} & = & \mu\left(\dfrac{1}{r}\dfrac{\partial v_r}{\partial \theta} + \dfrac{\partial v_\theta}{\partial r} - \dfrac{v_\theta}{r}\right), & \text{in } [0, R] \times [0, 2\pi], \\
\sigma_{rr} = 0, \ \sigma_{r\theta} = 0, & & & \text{in } R \times [0, 2\pi],
\end{array}\right. \tag{63}$$

with the initial conditions

$$v_s((r, \theta), t = 0) \ = \ 0.1F(\frac{r}{r_0}), \quad s \in \{r, \theta\}, \tag{64}$$

we remark that the solution depends only on r and the former equations are equivalent to the two following decoupled one dimensional problems:

$$
\left|\begin{array}{rcll}
\rho\dfrac{\partial v_r}{\partial t} & = & \dfrac{\partial \sigma_{rr}}{\partial r} + \dfrac{1}{r}(\sigma_{rr}-\sigma_{\theta\theta}), & \text{in } [0,R], \\
\dfrac{\partial \sigma_{rr}}{\partial t} & = & (2\mu+\lambda)\dfrac{\partial v_r}{\partial r} + \lambda\dfrac{v_r}{r}, & \text{in } [0,R], \\
\dfrac{\partial \sigma_{\theta\theta}}{\partial t} & = & (2\mu+\lambda)\dfrac{v_r}{r} + \lambda\dfrac{\partial v_r}{\partial r}, & \text{in } [0,R], \\
\sigma_{rr} & = & 0, & \text{in } R,
\end{array}\right. \tag{65}
$$

$$
\left|\begin{array}{rcll}
\rho\dfrac{\partial v_\theta}{\partial t} & = & \dfrac{\partial \sigma_{r\theta}}{\partial r} + \dfrac{2}{r}\sigma_{r\theta}, & \text{in } [0,R]\times[0,2\pi], \\
\dfrac{\partial \sigma_{r\theta}}{\partial t} & = & \mu\left(\dfrac{\partial v_\theta}{\partial r} - \dfrac{v_\theta}{r}\right), & \text{in } [0,R]\times[0,2\pi], \\
\sigma_{r\theta} & = & 0, & \text{in } R\times[0,2\pi].
\end{array}\right. \tag{66}
$$

We solve numerically those systems using piecewise constant functions for the discretization of the velocity field and continuous linear functions for the stress tensor. For the time discretization we use a leap frog scheme. The reference solution is obtained using a very fine mesh ($h_{1d} \approx 1/800$). The two dimensional problem is solved using four different meshes with $h_z = h_z = 1/10, 1/20, 1/40$ and $1/80$. We use the larger time step Δt authorized by the CFL condition. The mesh for the object is uniform and with a discretization step H such that $H/h \approx 4$ for each mesh. In all cases the damping parameter β is equal to zero. For each numerical experiment we compute the difference between the approximated solution and the reference solution. In figure 14 we display the logarithm of the error on the stress tensor, the velocity field and the Lagrange multiplier versus the logarithm of the discretization step. The rate of convergence is thus given by the slope of the lines. We observe that the order of convergence for σ in $L^\infty([0,T],(H(div,C))^2)$ norm and for $\mathbf{v}$ in $L^\infty([0,T],(L^2(C))^2)$ norm are near from the values we could expect (i.e. $1/2$), while for λ in $L^\infty([0,T],(L^2(\Gamma))^2)$ it is better (around 1 instead of $1/2$), which we explain to be related to the closed boundary, as in the scalar case.

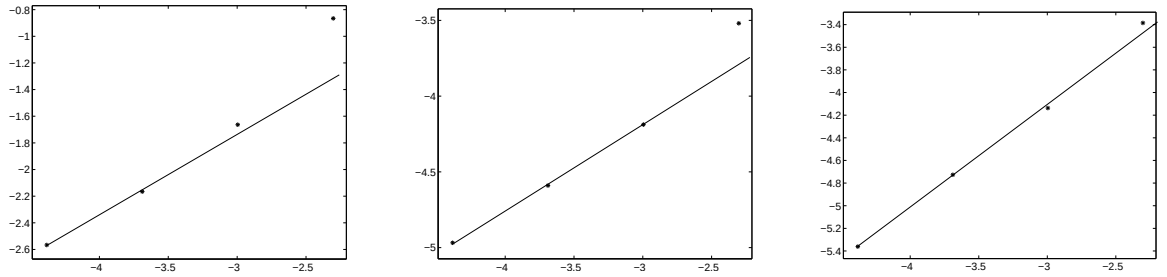

(a) $\sup_{t\le T} \|\boldsymbol{\sigma}-\boldsymbol{\sigma}_h\|_{\underline{\underline{X}}}$, $s = 0.59$ (b) $\sup_{t\le T} \|\mathbf{v}-\mathbf{v}_h\|_{\underline{M}}$, $s = 0.55$ (c) $\sup_{t\le T} \|\boldsymbol{\lambda}-\boldsymbol{\lambda}_h\|_{\underline{\mathcal{G}}}$, $s = 0.92$

Figure 14: Numerical error on $\boldsymbol{\sigma}$, $\mathbf{v}$ and $\boldsymbol{\lambda}$ versus the discretization step.

In figure 15 we represent the logarithm of the errors on the stress tensor and the velocity field measured on $\widetilde{C} = C \setminus B_{0.15}(\Gamma)$. As in the scalar case we recover the order of convergence of the method without obstacle (i.e. O(h) here) where we remove a neighborhood of the object in which the solution is not very smooth.

Finally we discuss the influence of the damping parameter β on the convergence results. In order to do so we repeat the experiment described above using the mesh with $h = 1/40$ mm for $\beta/\rho 10^{-6} = 0, 0.5, 2.5, 5, 7.5, 10, 12.5$ and 15 . We display on figure 16 the logarithm of the error on $\boldsymbol{\sigma}$, $\mathbf{v}$ and $\boldsymbol{\lambda}$ as a function of the value of $\beta/\rho 10^{-6}$.

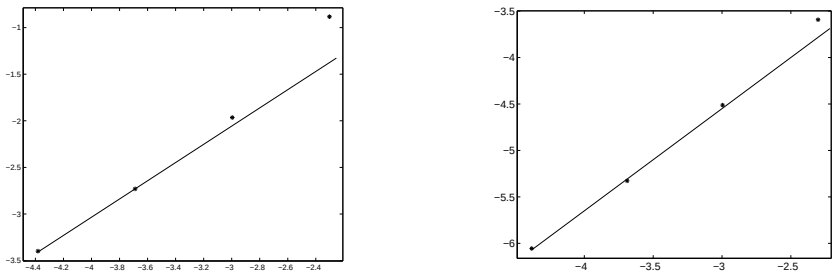

(a) $\sup_{t\leq T} \|\boldsymbol{\sigma} - \boldsymbol{\sigma}_h\|_{\underline{\underline{H_{div}}}(\widetilde{C})}$. $s = 0.96$. (b) $\sup_{t\leq T} \|\mathbf{v} - \mathbf{v}_h\|_{\underline{L^2}(\widetilde{C})}$. $s = 1.05$.

Figure 15: Numerical error $\boldsymbol{\sigma}$, $\mathbf{v}$ versus the discretization step. Here we compute the norm of the error on $\widetilde{C}$.

As we can see, better results are obtained for values of $\beta/\rho 10^{-6}$ between 2.5 and 5. We also observe that the error increases when we choose β too large. The same experiments done for different materials show that the optimal range for β/ρ is independant of the material. It depends only on the number of points per wavelength in the discretization. It should be proportional to $1/\Delta t$:

$$\frac{\beta}{\rho} = \frac{\zeta}{\Delta t}$$

where ζ, an adimensional constant, determined by the previous experiment, should be chosen in the interval $[0.03, 0.06]$.

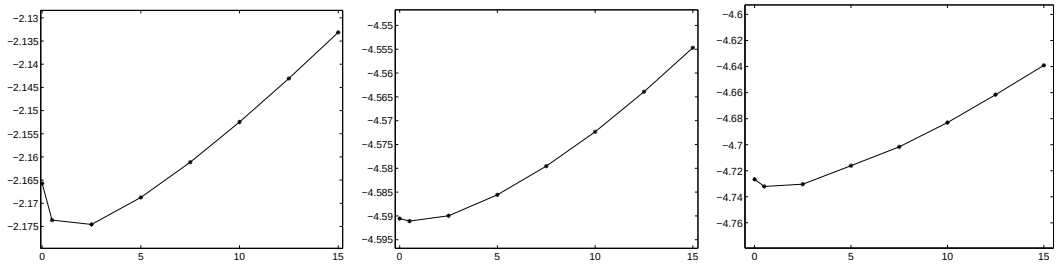

(a) $\sup_{t\leq T} \|\boldsymbol{\sigma} - \boldsymbol{\sigma}_h\|_{\underline{\underline{X}}}$. (b) $\sup_{t\leq T} \|\mathbf{v} - \mathbf{v}_h\|_{\underline{M}}$. (c) $\sup_{t\leq T} \|\boldsymbol{\lambda} - \boldsymbol{\lambda}_h\|_{\underline{\mathcal{G}}}$.

Figure 16: Numerical error on $\boldsymbol{\sigma}$, $\mathbf{v}$ and $\boldsymbol{\lambda}$ versus the damping parameter β/ρ.

Conclusion

We consider in this paper the application of the fictitious domain method for taking into account the Neumann boundary condition on the surface of a crack (or more generally an object) in the context of acoustic and elastic wave propagation. We first demonstrate with numerical examples that the method introduced in [5] does not converge for all crack geometries. We propose instead the use of a modified version of the mixed finite elements introduced in [4, 6]. Those elements consist in enriching the approximation space for the primal unknown. We carried out the theoretical and numerical convergence analysis of the method in the acoustic case. In the elastic case, although not obtained theoretically, the convergence of the method is verified through extensive numerical

simulations. In both cases (acoustic and elastic) the numerical results also indicate the introduction of spurious propagating modes (non-physical waves) due the enrichment of the approximation space. One way, for facing this difficulty is to introduce artificial absorption to damp these spurious modes. We propose a way for choosing the damping coefficient in order not to affect the physical part of the solution.

References

[1] I. BABUSKA, *The Finite Element Method with Lagrangian Multipliers*, Numer. Math., 20 (1973), pp. 179–192.

[2] E. BÉCACHE, A. CHAIGNE, G. DERVEAUX, AND P. JOLY, *Time-domain simulation of a guitar: Model and method.*, J. Acoust. Soc. Am., 6 (2003), pp. 3368 – 3383.

[3] E. BÉCACHE, P. JOLY, AND C. TSOGKA, *Eléments finis mixtes et condensation de masse en élastodynamique linéaire. (i) construction*, C.R. Acad. Sci. Paris, t. 325, Série I (1997), pp. 545–550.

[4] ——, *An analysis of new mixed finite elements for the approximation of wave propagation problems*, SINUM, 37 (2000), pp. 1053–1084.

[5] ——, *Fictitious domains, mixed finite elements and perfectly matched layers for 2d elastic wave propagation*, J. of Comp. Acous, 9 (2001), pp. 1175–1203.

[6] ——, *A new family of mixed finite elements for the linear elastodynamic problem*, SINUM, 39 (2002), pp. 2109–2132.

[7] J. P. BÉRENGER, *A Perfectly Matched Layer for the Absorption of Electromagnetic Waves*, J. of Comp. Phys., 114 (1994), pp. 185–200.

[8] F. BREZZI AND M. FORTIN, *Mixed and Hybrid Finite Element Methods*, Springer-Verlag, New York, 1991.

[9] GARY COHEN, *Higher-order numerical methods for transient wave equations*, Scientific Computation, Springer-Verlag, Berlin, 2002. With a foreword by R. Glowinski.

[10] F. COLLINO, P. JOLY, AND F. MILLOT, *Fictitious domain method for unsteady problems: Application to Electromagnetic scattering*, J.C.P, 138 (1997), pp. 907–938.

[11] F. COLLINO AND C. TSOGKA, *Application of the PML Absorbing Layer Model to the Linear Elastodynamic Problem in Anisotropic Heteregeneous Media*, Geophysics, 66 (2001), pp. 294–307.

[12] S. GARCÈS, *Application des méthodes de domaines fictifs à la modélisation des structures rayonnantes tridimensionnelles*, PhD thesis, 1998.

[13] V. GIRAULT AND R. GLOWINSKI, *Error analysis of a fictitious domain method applied to a Dirichlet problem*, Japan J. Indust. Appl. Math., 12 (1995), pp. 487–514.

[14] VIVETTE GIRAULT AND PIERRE-ARNAUD RAVIART, *Finite element methods for Navier-Stokes equations*, vol. 5 of Springer Series in Computational Mathematics, Springer-Verlag, Berlin, 1986. Theory and algorithms.

[15] ROLAND GLOWINSKI AND YURI KUZNETSOV, *On the solution of the Dirichlet problem for linear elliptic operators by a distributed Lagrange multiplier method*, C. R. Acad. Sci. Paris Sér. I Math., 327 (1998), pp. 693–698.

[16] R. GLOWINSKI, T.W. PAN, AND J. PERIAUX, *A fictitious domain method for Dirichlet problem and applications*, Comp. Meth. in Appl. Mech. and Eng., 111 (1994), pp. 283–303.

[17] P. GRISVARD, *Problèmes aux limites dans les polygones. Mode d'emploi*, EDF.

[18] ERKKI HEIKKOLA, YURI A. KUZNETSOV, PEKKA NEITTAANMÄKI, AND JARI TOIVANEN, *Fictitious domain methods for the numerical solution of two-dimensional scattering problems*, J. Comput. Phys., 145 (1998), pp. 89–109.

[19] ERKKI HEIKKOLA, TUOMO ROSSI, AND JARI TOIVANEN, *A domain embedding method for scattering problems with an absorbing boundary or a perfectly matched layer*, J. Comput. Acoust., 11 (2003), pp. 159–174. Medium-frequency acoustics.

[20] P. JOLY AND L. RHAOUTI, *Analyse numérique - Domaines fictifs, éléments finis H(div) et condition de Neumann : le problème de la condition inf-sup* , C.R. Acad. Sci. Paris, 328, Série I (1999), pp. 1225–1230.

[21] YU. A. KUZNETSOV, *Fictitious component and domain decomposition methods for the solution of eigenvalue problems*, in Computing methods in applied sciences and engineering, VII (Versailles, 1985), North-Holland, Amsterdam, 1986, pp. 155–172.

[22] J.C. NÉDÉLEC, *A new family of mixed finite elements in* $\mathbb{R}^3$, Numer. Math., 50 (1986), pp. 57–81.

[23] L. RHAOUTI, *Domaines fictifs pour la modélisation d'un probème d' interaction fluide-structure: simulation de la timbale*, PhD thesis, Paris IX, 1999.

[24] N. TORDJMAN, *Eléments finis d'ordre élevé avec condensation de masse pour l'équation des ondes*, PhD thesis, Univ. Paris IX, 1995.

Unité de recherche INRIA Rocquencourt
Domaine de Voluceau - Rocquencourt - BP 105 - 78153 Le Chesnay Cedex (France)

Unité de recherche INRIA Futurs : Parc Club Orsay Université - ZAC des Vignes
4, rue Jacques Monod - 91893 ORSAY Cedex (France)
Unité de recherche INRIA Lorraine : LORIA, Technopôle de Nancy-Brabois - Campus scientifi que
615, rue du Jardin Botanique - BP 101 - 54602 Villers-lès-Nancy Cedex (France)
Unité de recherche INRIA Rennes : IRISA, Campus universitaire de Beaulieu - 35042 Rennes Cedex (France)
Unité de recherche INRIA Rhône-Alpes : 655, avenue de l'Europe - 38334 Montbonnot Saint-Ismier (France)
Unité de recherche INRIA Sophia Antipolis : 2004, route des Lucioles - BP 93 - 06902 Sophia Antipolis Cedex (France)

Éditeur
INRIA - Domaine de Voluceau - Rocquencourt, BP 105 - 78153 Le Chesnay Cedex (France)
http://www.inria.fr
ISSN 0249-6399